Final Report

on

Study of Cryogenic Plasma in Superfluid Liquid Helium

AOARD-04-4018

For the period of
June 7, 2004 to August 6, 2005

Submitted to

Dr. Misoon Y. Mah

Program Manager, AOARD

Unit 45002, APO AP 96337-5002
7-23-17 Roppongi, Minato-ku
Tokyo 106-0032 Japan

Submitted on August 23, 2005

By

Osamu Ishihara, Principal Investigator
Professor, Department of Physics
Faculty of Engineering
Yokohama National University, Yokohama 240-8501 Japan
Tel/Fax 045-339-4183
oishihar@ynu.ac.jp

Report Documentation Page

Form Approved
OMB No. 0704-0188

1. REPORT DATE	2. REPORT TYPE	3. DATES COVERED
26 JUL 2006	**Final Report (Technical)**	**07-06-2004 to 24-03-2006**

4. TITLE AND SUBTITLE	5a. CONTRACT NUMBER
Study of Cryogenic Plasma in Superfluid Liquid Helium	**FA520904P0393**
	5b. GRANT NUMBER
	5c. PROGRAM ELEMENT NUMBER
6. AUTHOR(S)	5d. PROJECT NUMBER
Osamu Ishihara	5e. TASK NUMBER
	5f. WORK UNIT NUMBER
7. PERFORMING ORGANIZATION NAME(S) AND ADDRESS(ES)	8. PERFORMING ORGANIZATION REPORT NUMBER
Department of Physics, Faculty of Engineering,79-5 Tokiwadai Hodogaya,Yokohama 240-8501,NA,JAPAN	**AOARD-044018**
9. SPONSORING/MONITORING AGENCY NAME(S) AND ADDRESS(ES)	10. SPONSOR/MONITOR'S ACRONYM(S)
The US Resarch Labolatory, AOARD/AFOSR, Unit 45002, APO, AP, 96337-5002	**AOARD/AFOSR**
	11. SPONSOR/MONITOR'S REPORT NUMBER(S) **AOARD-044018**

12. DISTRIBUTION/AVAILABILITY STATEMENT

Approved for public release; distribution unlimited

13. SUPPLEMENTARY NOTES

14. ABSTRACT

The work describes work on Study of Cryogenic Plasma in Superfluid Liquid Helium (Principal investigator: O. Ishihara, AOARD-04-4018) for the period from June 7, 2004 to August 6, 2005. A preliminary experiment to produce a DC discharge plasma in a vapor of liquid helium started. In addition, a complex plasma with charged fine particles in the cryogenic environment has been also produced successfully. The analytical study on the experimental results completed at Niigata University for the pulsed discharge in a microwave cavity in liquid helium revealed the nature of decaying plasma in liquid helium.

15. SUBJECT TERMS

Plasma Physics, Plasma Dynamics, Plasma Sources, Quantum Physics, Pulsed Power

16. SECURITY CLASSIFICATION OF:			17. LIMITATION OF ABSTRACT	18. NUMBER OF PAGES	19a. NAME OF RESPONSIBLE PERSON
a. REPORT	b. ABSTRACT	c. THIS PAGE			
unclassified	**unclassified**	**unclassified**		**31**	

SUMMARY

This Final Report describes the research work on the contract of investigation entitled by Study of Cryogenic Plasma in Superfluid Liquid Helium (Principal investigator: O. Ishihara, AOARD-04-4018) for the period from June 7, 2004 to August 6, 2005. The research has been carried out at Yokohama National University in collaboration with Prof. K. Minami of Tokyo Denki University, a research associate Dr. Masako Shindo, a doctoral student Mr. Chikara Kijima, and two master students. A preliminary experiment to produce a DC discharge plasma in a vapor of liquid helium started and a complex plasma with charged fine particles in the cryogenic environment has been produced successfully. The analytical study on the experimental results completed at Niigata University for the pulsed discharge in a microwave cavity in liquid helium revealed the nature of decaying plasma in liquid helium.

I. Objectives

Our overall goal is to study the cryogenic plasma experimentally and theoretically and to reveal novel natures of cryogenic plasma produced by a pulsed or a DC discharge above or in superfluid liquid helium .

II. Status of the Research

(1) Preparation of the Dewar Bottles

The Physics Department in the faculty of engineering at Yokohama National University was established in 1998 and the principal investigator Osamu Ishihara joined the faculty of Yokohama National University in June of 1999. The plasma lab was established in the August of 2000 immediately after the completion of the new departmental building. Initially, major efforts in the research were devoted to the theoretical and computational plasma physics. The collaboration with Prof. K. Minami of Niigata University started in 2000 and the AOARD funding started in 2002 (AOARD-00-4014, Study of cryogenic plasma produced by a pulsed discharge in Superfluid liquid helium). The plasma lab expanded in space and the complex plasma experimental lab in the Department of Physics at Yokohama National University was established in March 2004.

The principal investigator, Professor Osamu Ishihara, has been conducting the research in collaboration with Dr. Masako Shindo, Research Associate joined in the group in April of 2002, and a doctoral student Mr. Chikara Kojima who joined in the group in April of 2004 and two master students, Mr. M. Kugue and Mr. T. Maesawa. Professor Kazuo Minami, retired from Niigata University and now with Tokyo Denki University, is consulting us on the research.

Following the retirement of Professor Minami from Niigata University in March, 2004,

a cryostat system including a Dewar vessel was transferred to Yokohama National University. A preliminary DC discharge in the vapor of liquid helium in the Dewar bottle was performed and preliminary probe measurements have been carried out. The setup is schematically shown in Fig. 1, where two thin-walled bottles nested one inside the other and the outer bottle is sealed at the ends. The one end of the inner bottle needs to be pumped to maintain the vacuum for insulation. The DC discharge in a vapor of liquid helium was accomplished by applying about 400V between a meshed stainless anode and a stainless disk cathode separated by 6 mm. The plasma was characterized by the electron temperature about 0.3 eV and the plasma density about $4\times10^{7}\,\mathrm{cm}^{-3}$. We note that the temperature of He vapor in the Dewar increased up to 86K during the discharge.

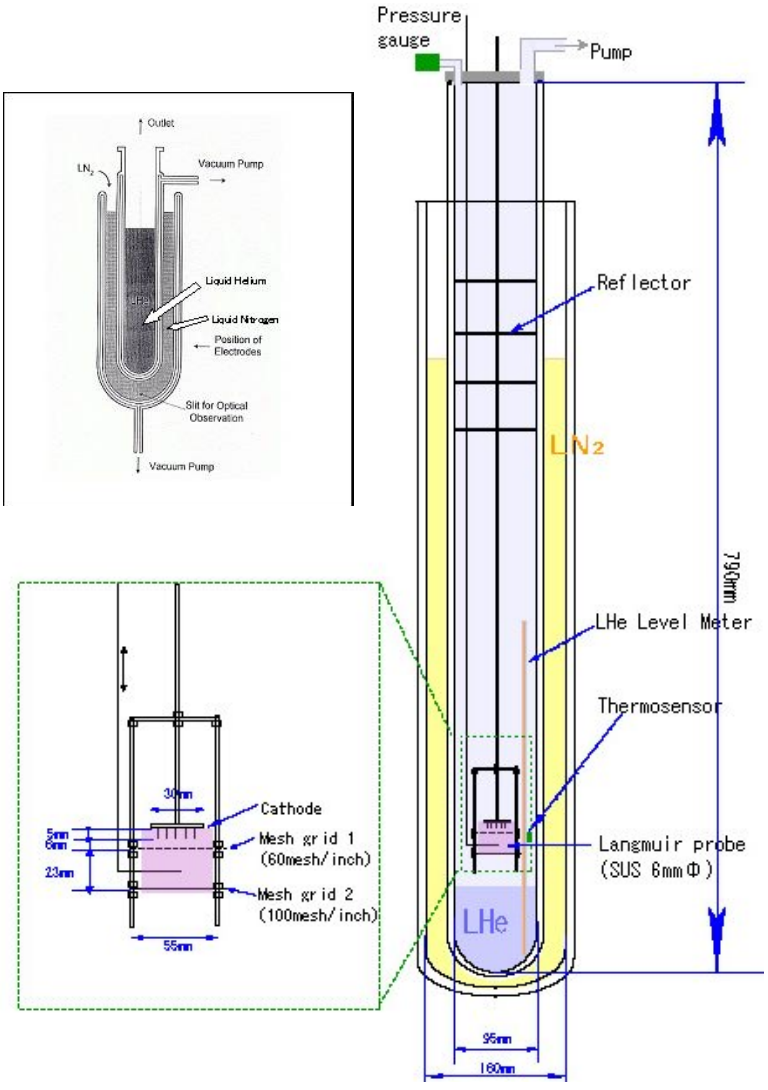

Fig.1 Schematic diagram of the experimental apparatus. A Dewar bottle has two thin-walled bottles nested one inside the other and the outer bottle is sealed at the ends. The electrodes are set above the liquid helium (LHe).

A larger Dewar vessel to accommodate a DC discharge chamber was designed, ordered and delivered. It is aimed to produce a plasma in a vapor of liquid helium in a confined chamber which is immersed in the liquid helium rather than in a vapor of liquid helium. Since the delivered vessel had a defect, the vessel had to be repaired at the JEC-Tori Corporation of Saitama Prefecture. While the Dewar vessel used in Niigata is rather small, 10 cm in inner diameter, the new Dewar vessel is 16cm in inner diameter to accommodate a DC discharge chamber of 10 cm in diameter. The Dewar vessel, as shown in Fig. 2, has two thin-walled bottles nested one inside the other and both bottles are sealed at the ends. A DC discharge chamber, to be immersed in the liquid helium, was designed ordered and delivered, while the original chamber delivered needed to get fixed due to a defect at an injection valve found later. The JEC Tori Corporation repaired the discharge chamber and delivered the chamber to us.

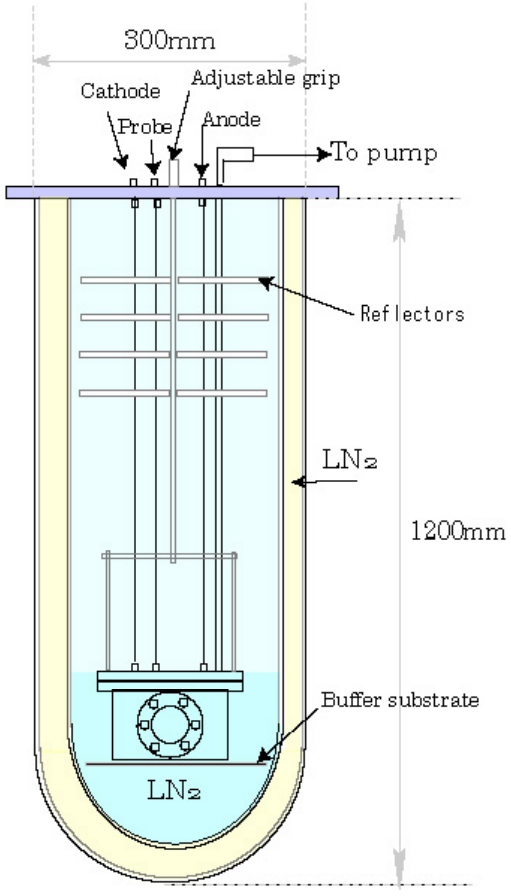

Fig. 2 A larger Dewar vessel, designed and constructed at Yokohama National University with a DC discharge chamber.

(2) Discharge in a chamber placed in the Dewar vessel

A preliminary discharge between a brass rod cathode and a brass rod anode in the DC discharge chamber, placed in the Dewar vessel, produced a plasma in a helium gas of 0.5 Torr maintained to be 77K by the heat exchange through the chamber wall. The electrodes, both 10mm in diameter and 40mm in length, were placed 10 mm apart in the chamber and were applied with the DC voltage of about 600 V. When the chamber was immersed in liquid nitrogen in the Dewar vessel, liquid nitrogen instead of liquid helium at a preliminary stage, the produced plasma was rather unstable to maintain the constant density. A Langmuir probe with 0.5 mm in diameter and 10 mm in length measured the electron temperature of order 1 eV and revealed the slight decrease in electron temperature in the presence of liquid nitrogen around the DC chamber compared with the electron temperature without liquid nitrogen. While we introduced liquid helium into the DC chamber, a leakage was found at a valve attached at the top of the DC chamber to introduce liquid helium. Our efforts to produce a stable plasma in a vapor of liquid helium continue and the plasma parameters have been measured yet with insufficient accuracy.

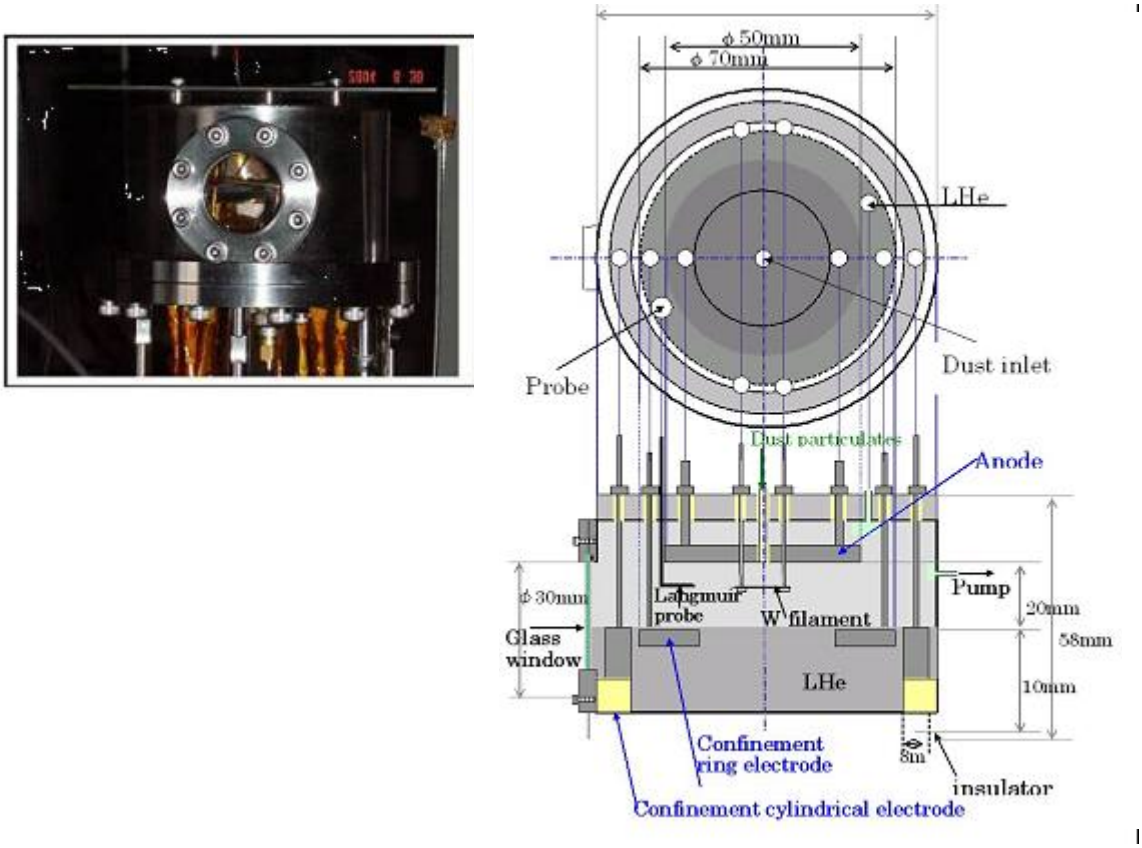

Fig. 3 DC discharge chamber to accommodate liquid helium (LHe) and to be immersed in liquid helium in the Dewar.

(3) Production of a steady state plasma in a vapor of the liquid helium

A cryogenic plasma in a steady state has been established by an electrical discharge (AC10kHz, ～1kV) in a vapor (2 Torr) above the liquid helium surface. The electrical discharge in the vapor necessarily brings a heat in the environment resulting in the boiling of the liquid helium. To overcome the rise of the surrounding plasma temperature as well as the instability of the surface of the liquid helium, a special purpose discharge unit has been developed. The unit is characterized by a region of plasma production isolated from the surroundings by a small glass Dewar. Two identical plane discharge electrodes have coaxial holes at the center through which the helium gas was fed from the upper hole. A plasma is produced by a discharge between the electrodes and the gas flow takes the plasma outside of the discharge region through the bottom hole. The rise of the plasma temperature once outside of the small glass Dewar is successfully suppressed and the plasma temperature decreases toward the surface of the liquid helium. The cold plasma in a steady state is thus successfully produced. The first report on this subject will be presented by a doctoral student Mr. Chikara Kojima at the domestic meeting in September (see Appendix 3).

(4) Complex plasma in the ultra-cold environment

A complex plasma is characterized by a group of negatively charged macro particles embedded in a plasma. The group of fine particles shows collective behaviors, while plasma particles show collective behavior independently with a time scale much faster and a space scale much shorter than those for the group of fine particles. The complex system including fine particles in a plasma is characterized by the unique interaction of the two collective modes. The fine particles (often called dust particles) are strongly coupled through Coulomb interaction with a large coupling constant Γ defined by the ratio of the Coulomb energy and the thermal energy of particles:

$$\Gamma = \frac{\text{Coulomb Energy}}{\text{Thermal Energy}} = \frac{(Z_d e)^2}{4\pi\varepsilon_0 r \kappa T_d},$$

where $Z_d e$ is the charge on the surface of a fine particle, r is the average inter-particle distance, κ is the Boltzmann constant, and T_d is the temperature of fine particles. We used here the subscript d for dust particles (fine particles). Ordinary plasmas with electrons and ions are characterized by rather a small coupling constant, $\Gamma << 1$, since the kinetic energy of plasma particles are dominant over the Coulomb energy allowing the random motion of plasma particles. The coupling constant for fine particles could be much larger than 1, either through $|Z_d| >> 1$ or $\kappa T_d \to 0$.

In an extremely low temperature environment, the thermal energy of the particles are suppressed resulting in a large coupling constant. We have injected fine acrylic particles of 5μm in diameter in a vapor above liquid helium at about 1K. The pressure measured at the

upper part of the Dewar was about 2 Torr. The discharge electrodes were set 200mm above the surface of liquid helium, and the distance between electrodes was 5mm. The 10kHz AC voltage of 1kV was applied to the driving electrodes. The surrounding of electrodes were covered by the insulator to suppress the rapid rise of the temperature of both liquid helium and the vapor gas. The produced plasma was diffused toward Liquid helium surface through a 5mm hole in lower electrode. It was confirmed that an electron temperature in the diffusion region decreased due to the presence of liquid helium by double probe measurements. The acrylic particles were dropped from the upper part into plasma through the 5mm holes at the center of the electrodes. They are expected to be charged negatively and blew out into the diffusion region. The diffusion region was covered with an acrylic tube of 50mm in diameter to confine the particle in the radial direction, and a negatively-biased plate electrode of 50mm in diameter was set 100mm under the discharge electrodes. The He-Ne laser light was irradiated from outside though a 10mm-width slit on the glass Dewar, which was silver plated except for the slit area, and the acrylic particles float 10mm above the plate electrodes in a plasma. The preliminary results will be presented in the coming Fall meeting of the Physical Society of Japan by a research associate Dr. Masako Shindo (See Appendix 3).

(5) Study of the equation of state

We have shown that the long-range interaction energy between fine particles placed in the plasma exhibits a unique feature with a repulsive nature for short distances and with an attractive nature for larger distances as shown in Fig. 4 (O. Ishihara and N. Sato, Attractive Force on Like Charges in a Complex Plasma, Physics of Plasmas, **12**, 070705 (2005), see Appendix 4). Such a finding suggests the possibility of the phase transition in the complex plasma. Although the topic of the equation of the state was not originally included in the proposal, the study of dusty plasmas prompted us to direct our attention to the equation of state applied to a complex plasma in a cryogenic environment. The long range interaction energy was formulated by the consideration of free energy available in the complex plasma where the charge neutrality is satisfied by the presence of electrons, ions, and the charged fine particles. With the explicit formulation of the interaction energy, the second Virial coefficient will be calculated. And the equation of state will give us a clue to the study of the critical phenomenon in the complex plasma. The possible presence of a critical point in the complex plasma in the cryogenic environment is still an open question both theoretically and experimentally.

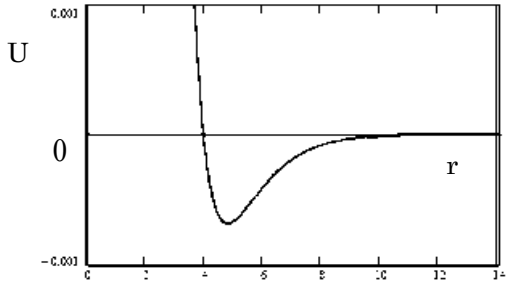

Fig. 4 Interaction energy of fine particles in a complex plasma.

(6) Analysis of the ultracold plasma produced by a pulse discharge

After all the experiments at Niigata University completed, the data taken for the pulsed discharge were analyzed through the initiative of Professor Minami. Our focus was on the understanding of the decaying plasma produced by a high-voltage (~20kV) pulse of duration on the order of micro seconds in an X-band mode cylindrical cavity filled with Liquid helium. Although the transmission signals through the cavity show clearly the presence of decaying plasma in liquid helium with decay time on the order of a few hundred ms for temperature of a few K at saturating vapor pressure, our estimated mass of charged carriers seems to be much less than expected from the earlier theoretical predictions. The paper is now in print (see Appendix 1) and the results were presented at the international conference (see Appendix 2).

III. Publications/ Presentations

1. Publication (Appendix 1)

K. Minami, C. Kojima, and O. Ishihara, Microwave measurement of Decaying Plasma in Liquid Helium, IEEE Transaction on Plasma Science, August issue (2005).

2. International Conference Proceeding (Appendix 2)

C. Kojima, O. Ishihara, and K. Minami, Study of Decaying Plasma in Liquid Helium, 19th International Conference on Numerical Simulation of Plasmas and 7th Asian Pacific Plasma Theory Conference (July 12-15, 2005, Nara, Japan) P1-65, pp.151-152.

3. Domestic Conference Abstracts (Appendix 3)

M. Shindo, C. Kojima, O. Ishihara, Observation of dust particles in a plasma under cryogenic environment, Fall Meeting, Physical Society of Japan (2005.9.19-22, Kyoto) 21 p WG-1 .

C. Kojima, M. Kugue, T. Maezawa, M. Shindo and O. Ishihara, A plasma production in a region of low temperature, Fall Meeting, Physical Society of Japan (2005.9.19-22, Kyoto) 22 aWG-2.

IV. AOARD site visits

August 6, 2004

AOARD program manager Dr. Misoon Y. Mah

September 24, 2004

AOARD program manager Dr. Misoon Y. Mah,

AOARD Science Advisor Dr. Takeo Miyazaki,

Air Force Research Laboratory (Kirtland AFB) Senior Research Physicist Dr. S. Joe Yakura

AF Research Laboratory (Kirtland AFB) Chief of Applications Branch Maj. Jeffrey C. Wiemeri

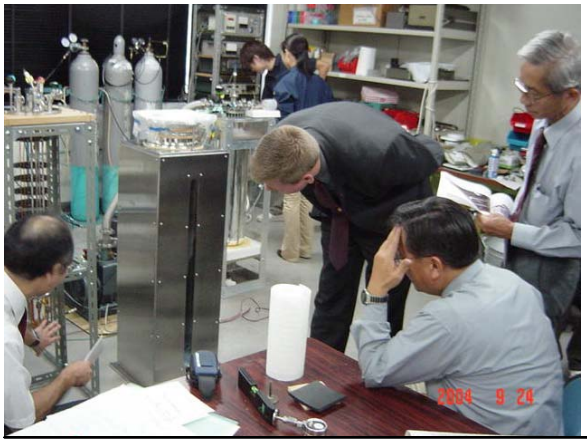

Maj. Wiemeri, Dr. Yakura, Dr. Mah, Dr. Miyazaki, Prof. Ishihara

V. Lab photos

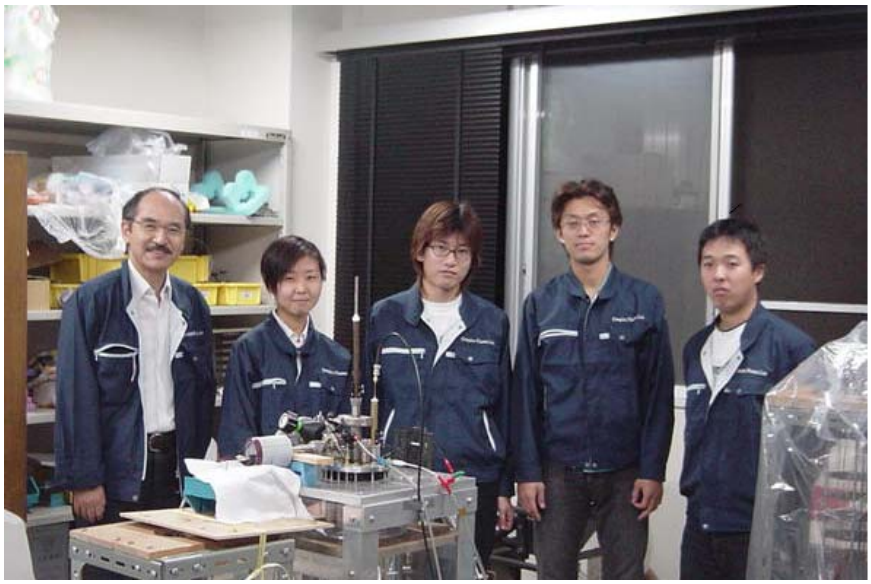

Osamu Ishihara, Masako Shindo and three graduate students

Professor Ishihara's lab was introduced in an annual campus guide YNU 2005.

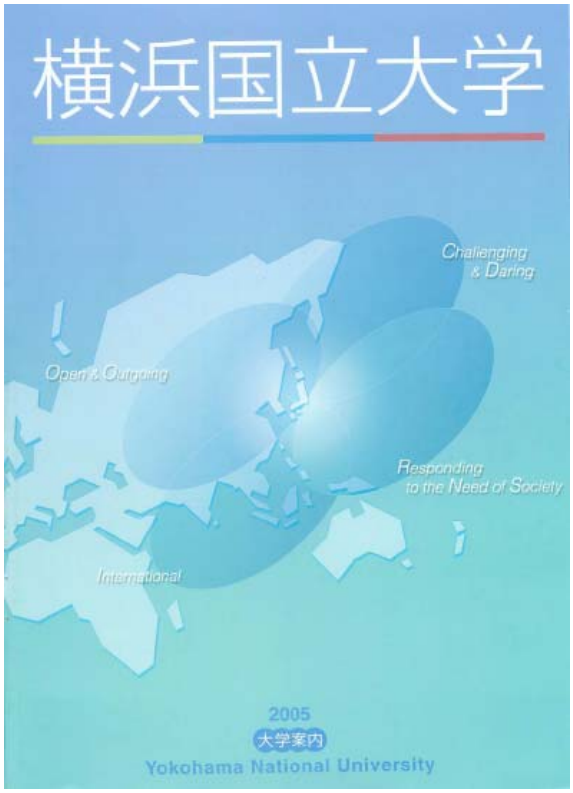

APPENDIX 1

To appear in August 2005 Issue of IEEE TPS.

Microwave Measurement of Decaying Plasma in Liquid Helium

Kazuo Minami, *Member, IEEE*, Chikara Kojima, Takeo Ohira, and Osamu Ishihara, *Fellow, IEEE*

***Abstract*—Decaying plasma in a microwave cavity filled with liquid helium (LHe, hereafter) is studied. An X-band TE_{113} mode cylindrical cavity is filled with LHe, and a high-voltage pulse with duration 7 μs, voltage V $\leq$ 20 kV, and current I $\leq$ 360 A is applied between a tungsten needle electrode and a thin stainless-steel mesh which separates an adjacent small discharge space from the cavity. The transmission signals through the cavity show the presence of decaying plasma in LHe with decay time on the order of 200 ms for a temperature range from 4.2 to 2.3 K at saturating vapor pressure. The response signals are suppressed in the pressurized LHe, as well as in superfluid LHe below 2.17 K. Our estimated mass of the charged carriers just after the pulsed discharge, assuming a diffusion loss mechanism, is much less than the value known as an effective mass of heavy ions which were produced by a steady-state ion source in LHe measured by Poitrenaud and Williams (1972). Our experimental observation suggests that the heavy effective mass of ions in LHe might take time to develop to its full extent.**

***Index Terms*—Cavity, cryogenic plasma, diffusion, electron bubbles, ion clusters, liquid helium, microwave, pulsed discharge, recombination, superfluid.**

I. Introduction

ULTRACOLD plasma is a new subject of research in plasma science that is currently in rapid progress. While a new technology including laser cooling has been utilized to produce an ultracold plasma [1], we have successfully produced cryogenic decaying plasma in liquid helium (LHe, hereafter), as well as in cryogenic gas helium with temperature below 4.2 K by means of a pulsed discharge [2]–[5]. Cryogenic plasma in LHe is known to be characterized by features such as electron bubbles and positive ion clusters [6]–[8]. In our earlier experiments, we succeeded in producing a high-density localized plasma in LHe. High-voltage pulsed discharge with needle electrodes in LHe produced the localized plasma with density more than 10^{18} cm^{-3} and electron and ion temperatures of a few electronvolts [2], [3]. Upon termination of the discharge, the plasma remained as long as on the order of 10 μs in LHe. Some of ions and electrons remained longer in LHe before they recombine [5]. Such a cryogenic plasma, or positive and negative ion (p-ion and n-ion, hereafter) mixture dissolved in LHe, is the subject of our interest in this paper. In our previous paper [4], a plasma in cryogenic helium gas in a TE_{011} mode S-band cavity with very long decay time on the order of 1 s was observed. In this paper, we apply the microwave cavity method to measure decaying plasma in LHe. Late afterglow plasma in an X-band cavity filled with LHe in the temperature range from 4.2 to 1.69 K is studied. Slow decaying plasmas in LHe detected as long as 200 ms after the discharge are reported in this paper. The plasma is observed in LHe at a saturating vapor pressure with temperature above 2.3 K. Although the cavity method may not be fully applicable to the present study because of the nature of the local plasma production, our estimated density based on the cavity method suggests an effective mass of ions much different from that expected by the conventional theory. A simple diffusion loss model for a temporal evolution of the localized plasma produced by the pulsed discharge in LHe reveals the presence of charged carriers with masses much lighter than those expected in LHe.

The organization of the paper is as follows. In Section II, the principle of cavity measurements that were used in our previous paper [4] are reviewed briefly. The experimental setup, procedure, and experimental results are described in Section III. In Section IV, expected temporal evolution of localized decaying plasma in LHe is analyzed to compare with the experimental results. Discussion and conclusion are given in Section V.

II. Principle of Cavity Measurements

In our previous paper on cryogenic gas plasma [4], cavity measurement was applied to detect the density n in the decaying plasma. The method is now extended to the measurement of localized plasma in LHe in an X-band cavity. The angular frequency ω of the sensing microwave is adjusted to be $\omega = \omega_0 + B_0$, as shown in Fig. 1 in [4], where ω_0 and B_0 are the resonant angular frequency of the cavity without plasma and half half-width of the resonant curve, as shown in Fig. 1 in [4]. The resonant frequency in the cavity will be shifted upward in the presence of plasma and the measured frequency shifting will determine the plasma density n. Fig. 2 in [4] is the microwave interferometer including the plasma loaded cavity. Two detected signals $u = |T|^2$ and $v = |T|\sin\varphi$ are displayed on a digital oscilloscope, where $|T|$ and φ are, respectively, the magnitude and the phase of the transmission coefficient through the plasma cavity. Assuming uniform plasma in the cavity, the plasma density n is expressed by [4]

$$n(m^{-3}) = A \cdot F \cdot \frac{B_0}{2\pi}\left(2 + \frac{1 - 2\sqrt{u - v^2}}{u + v}\right) \quad (1)$$

Manuscript received April 10, 2004; revised May 27, 2005. This work is supported in part by Asian Office of Aerospace Research and Development (AOARD) and by Grant-in-Aid for Scientific Research, Japan Society for Promotion of Science.

K. Minami, C. Kojima, and T. Ohira are with Graduate School of Science and Technology, Niigata University, Niigata, 950-2181 Japan (e-mail: kminami@msa.biglobe.ne.jp).

O. Ishihara is with Department of Physics, Yokohama National University, Yokohama, 240-8501 Japan (e-mail: oishihar@ynu.ac.jp).

Digital Object Identifier 10.1109/TPS.2005.852405

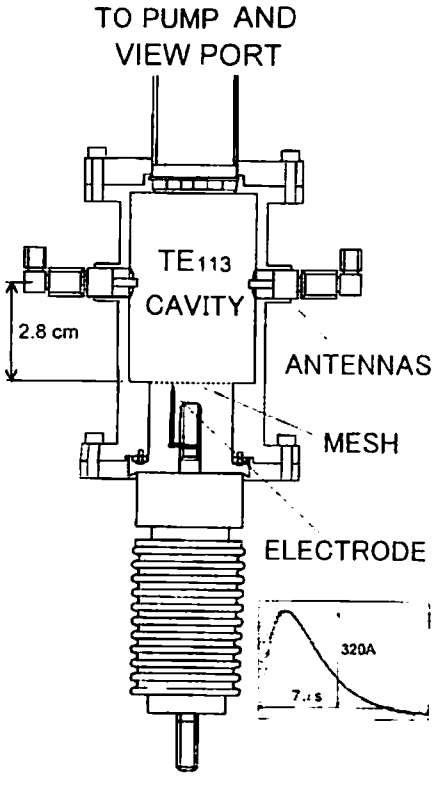

Fig. 1. Cross-sectional view of X-band TE_{113} mode plasma cavity. A thin stainless-steel mesh divides the cylindrical plasma container into the plasma cavity at the upper portion and the discharge chamber for plasma production at the lower portion. High-voltage pulse is applied at the terminal at the bottom. Inset shows a typical current waveform for pulsed discharge measured by a Rogowski coil. Distance between the position of plasma production and the antennas is 2.8 cm.

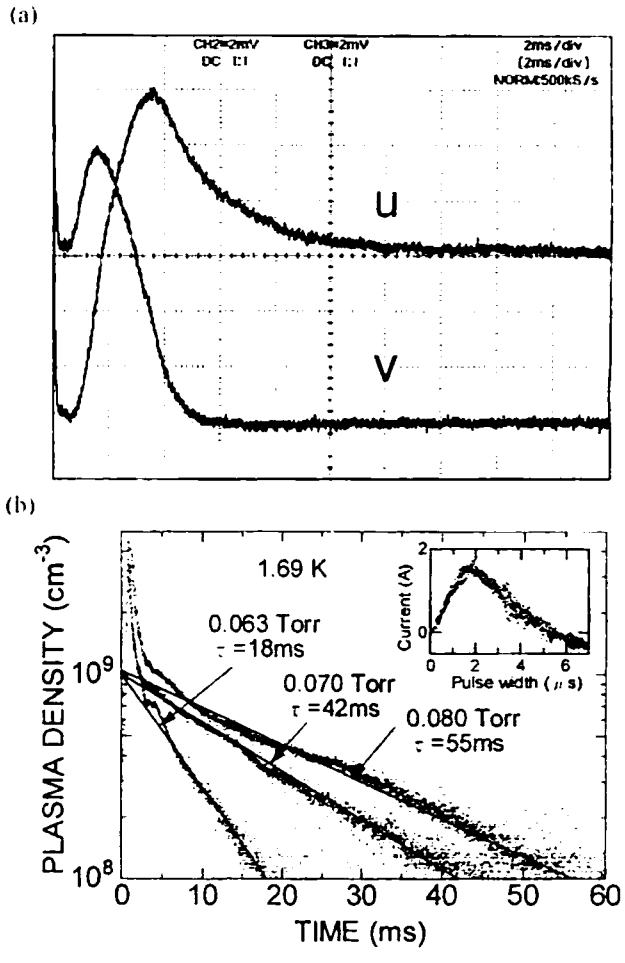

Fig. 2. Measurements in cryogenic helium gas with temperature 1.69 K and applied voltage less than 20 kV. (a) Trace of microwave signals u and v through the cavity when it is filled with cryogenic helium gas with pressure 0.3 torr. (b) Logarithmic plot of plasma density versus time when the cavity is filled with helium gas for three pressures 0.063, 0.070, and 0.080 torr. Inset shows the current waveform for pulsed discharge. Decay time constant and ambipolar diffusion coefficient are obtained from the fitted straight line.

where F is the sensing microwave angular frequency in gigahertz, $B_0/2\pi$ is the half half-width of the resonant curve of the cavity without plasma in megahertz, and

$$A = \frac{8\pi^2\varepsilon_0 m}{e^2} \times 10^{15} \tag{2}$$

is a constant with the mass m of charged carriers which respond to the microwave fields. In the case of gaseous plasma, m is the mass of an electron 9.11×10^{-31} kg, while the mass m in (2) may be given by the effective mass of a p-ion in LHe, or 2.67×10^{-25} kg [6]–[8], 40 times the mass of a ^{4}He atom that is smaller than the mass of n-ions. When the cavity is filled with LHe, the charged carriers responding to the microwave fields may be p-ions that have effective mass 2.9×10^5 times that of electrons, resulting in the constant $A = 7.29 \times 10^{18}$ in (2), while $A = 2.19 \times 10^{13}$ for the single electron mass. Using (1) and (2) with the measured signals u and v at each time after the pulsed discharge, one can obtain effective plasma density n averaged over the cavity. This is the methodology of the present cavity measurement of plasma in LHe.

III. Experiment

A. Experimental Setup and Procedure

The schematic cross section of the X-band stainless-steel cylindrical cavity for TE_{113} mode with resonant frequency 9.20 GHz is shown in Fig. 1. The sizes of the cavity are 3.6 cm inner diameter and 5.6 cm in length. A thin and flat stainless-steel mesh divides the cylindrical vessel into two portions: the upper for the plasma cavity of microwave measurement and the lower for the discharge chamber for plasma production. The mesh separates the cavity from the place of high-voltage pulse application to avoid the damage to the microwave measurement circuit. The wall and two antennas in the cavity are grounded to minimize induction noise caused by the high-voltage pulse. In the discharge chamber with an inner diameter 2.2 cm and the height 3.0 cm, the plasma is produced by single or repetitive shots of a high-voltage pulse between a tungsten needle electrode with tip curvature 50 μm and the stainless-steel mesh. The separation between the needle and the mesh is less than 1 mm. The pulse voltage can be varied from 16 to 20 kV. A typical wave form of a discharge current measured by a Rogowski coil is shown in the inset at right bottom of Fig. 1. The maximum discharge current is less than 360 A and the duration is 7 μs. While (1) is applicable only to a uniform plasma as in gas helium, we expect that the plasma density in LHe averaged over

the cavity volume in the late afterglow period may be evaluated reasonably, if the plasma frequency is less than the microwave frequency in the cavity.

The plasma cavity is connected to a microwave circuit by two semi-rigid cables (UT-141A) through a pair of antennas at the side wall. The locations and shapes of the antennas are fixed to obtain optimal performance for the measurements of the resonant cavity after many trials and error tests. Both antennas for input and output ports are roughly identical and located symmetrically. A CW Gunn oscillator with microwave power less than 1 mW is connected to the input antenna. The output antenna is connected to a coaxial detector (HP432B) and a mixer (Watkins–Johnson, M80C), as shown in Fig. 2 in [4]. The cavity is installed inside a LHe dewar of volume 50 L made of stainless-steel with an inner diameter 45 cm and the depth 53 cm. The LHe dewar is installed inside a vacuum container in a stainless-steel cryostat with a small-scale refrigerator to produce LHe a few liters per hour. The whole system including the TE_{113} cavity is evacuated by a 6-in turbo-molecular pump to a pressure less than 10^{-6} torr before operation of the refrigerator. Microwave measurements of plasma density are carried out for LHe with saturated vapor pressure and cryogenic helium gas at a temperature range from $T = 4.2$ to 1.69 K. There are five small-radius holes at the top wall of the cavity shown in Fig. 1. Through the holes, one can watch with a TV camera the brightness of the pulsed discharge through the viewing port at the top of the cryostat. The signal from the Rogowski coil for monitoring discharge current is used to trigger the traces on the digital oscilloscope to observe the waveforms of the signals u and v through the plasma cavity. In our experiment, the lower limit of temperature of 1.69 K is attained by a rotary pump (30 m^3/h) with evacuation cooling of the 50 L LHe dewar surrounding the plasma cavity. It takes 8 h to cool down the cavity from 4.2 to 1.69 K, and around 50% of 50 L LHe in the dewar must be evaporated to attain 2.0 K.

The resonant frequency is measured to be $\omega_0/2\pi = 9.00$–9.20 GHz and the loaded Q value of the TE_{113} mode cavity without plasma is determined as $Q = \omega_0/2B_0 \approx 1540$, as shown in Fig. 1 in [4]. Because of the slow variation in the signals u and v on the oscilloscope, the amplitudes of the signals and setting of the frequency at $\omega_0 + B_0$ have to be calibrated and adjusted before each shot.

B. Experimental Results

In Section III-B-1, the measurements of decaying plasma in cryogenic helium gas are described briefly, and the results on decaying plasma in LHe are reported in Section III-B-2.

1) Decaying Plasma in Cryogenic Helium Gas at $T = 4.2$–1.69 K: Fig. 2(a) shows waveforms of the signals u and v through the plasma cavity in which helium gas at a temperature 1.69 K and pressure 0.3 torr is filled. The two signals, $0 \le u \le 1.0$ and $-0.5 \le v \le 0.5$, are adjusted to the range of six vertical divisions, respectively. The temporal evolution of the logarithmic plasma density, calculated by (1), is shown in Fig. 2(b). The observed plasma density is in the range of $10^8 - 10^9$ cm^{-3}, while the decaying plasma in a cryogenic helium gas in a TE_{011} mode S-band cavity [4] was characterized by the density in the range of $10^6 - 10^7$ cm^{-3}. Ambipolar diffusion was identified to be the dominant loss mechanism of the decaying plasma in the S-band TE_{011} mode cavity. The present TE_{113} X-band cavity has a sensing frequency about three times larger and Q value about 1/3 times smaller than the S-band TE_{011} mode cavity. Because higher plasma densities are observed in the present experiment, we expect the plasma to decay by diffusion as well as by recombination. When the pressure is less than 0.085 torr, the loss mechanism is dominated by diffusion because of the large ambipolar diffusion coefficient, while the recombination would play a major role in the loss mechanism for the pressures higher than 0.085 torr. The temporal plasma decay is shown in Fig. 2(b) for pressures, 0.063, 0.070, and 0.080 torr at 1.69 K, where the current wave form is depicted in the inset. We note that the peak current, 1.8 A, is much less than that shown in the inset of Fig. 1 for the discharge in LHe. This is because the plasma production in the cryogenic gas is much easier than in LHe. As is shown in Fig. 2(b), the density decreases exponentially with time, suggesting the presence of the ambipolar diffusion. The decay time increases with pressure, as is expected by the increase in collision frequency between helium ions and neutral helium atoms. We evaluate the ambipolar diffusion coefficient D_a from the measured decay time τ through the relation $\tau = \Lambda^2/D_a$, where $\Lambda = [(2.405/R)^2 + (\pi/L)^2]^{-1/2} = 0.69$ cm with radius $R = 1.8$ cm and length $L = 5.6$ cm for the cylindrical cavity. The diffusion coefficients, thus obtained, are 26.5, 11.3, and 8.66 cm^2/s for 0.063, 0.070, and 0.080 torr, respectively. The ambipolar diffusion coefficients in a gas with pressure P may be given by $D_a = 540/P$ (cm^2/s) for the helium gas at 300 K (see Brown [9]). Assuming $D_aP = 540(T/300)^{3/2}$, with a gas temperature T in equilibrium $T = T_e = T_i = 1.69$ K and the momentum transfer collision cross-section 5.8×10^{-15} cm^2 between helium ions and neutral helium atoms, we find expected values of D_a to be 3.6, 3.3, and 2.9 cm^2/s at pressures 0.063, 0.070, and 0.080 torr, respectively. Although the observed values of D_a are somewhat larger than the expected values, a deviation might be caused by an additional loss of the plasma such as the expansion of the plasma through the stainless mesh from the cavity to the discharge chamber where the plasma was originally produced. The late afterglow plasma in the present cavity disappears faster than a case for plasma cavity enclosed completely with metal wall, as was discussed in [4].

Fig. 3(a) shows the temporal decay of plasma density at $T = 1.69$ K in helium gas for pressures larger than those shown in Fig. 2(b). The decay is slower for the case of 0.090 torr than the case of 0.220 torr. Such a pressure dependence does not agree with the diffusion process described by $D_aP = \text{const.}$, and we see that the decay lines are not straight lines in the semi-log plot, as shown in Fig. 3(a). We may conclude that the loss of the plasma is caused not by ambipolar diffusion, but by recombination [9], [10]. Fig. 3(b) shows the inverse of the plasma density in Fig. 3(a) versus time. The slope of the fitted straight lines gives the values of recombination coefficient α. Estimated α thus obtained are 1.9×10^{-7}, 2.8×10^{-7} and 7.0×10^{-7} cm^3/s for pressure 0.090, 0.145 and 0.220 torr, respectively. The observed recombination coefficient α decreases with temperature

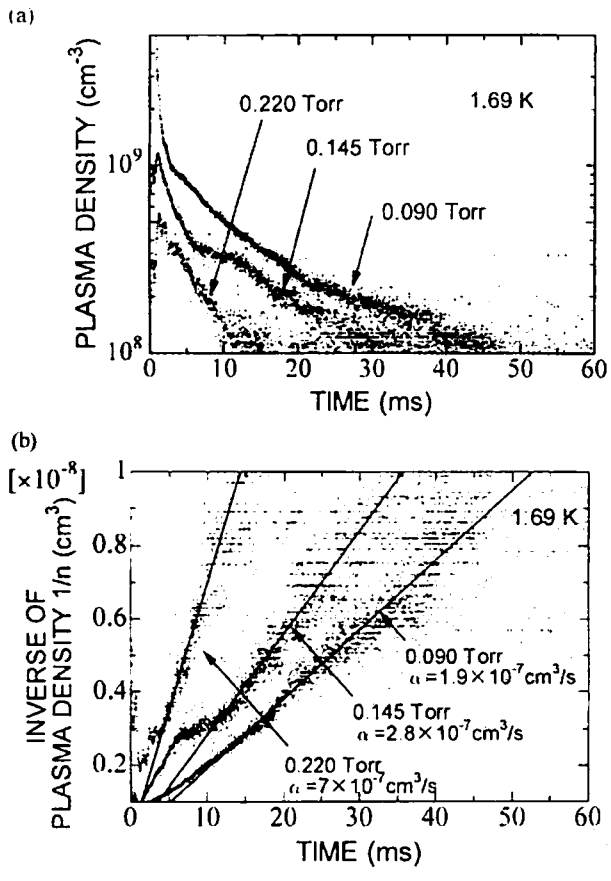

Fig. 3. Temporal evolution of the plasma density when the cavity is filled with helium gas at temperature 1.69 K for three gas pressures 0.090, 0.145, and 0.220 torr. Applied voltage is less than 20 kV. (a) Logarithmic plasma density versus time. (b) Inverse of plasma density versus time. Recombination coefficient is obtained from the fitted straight line.

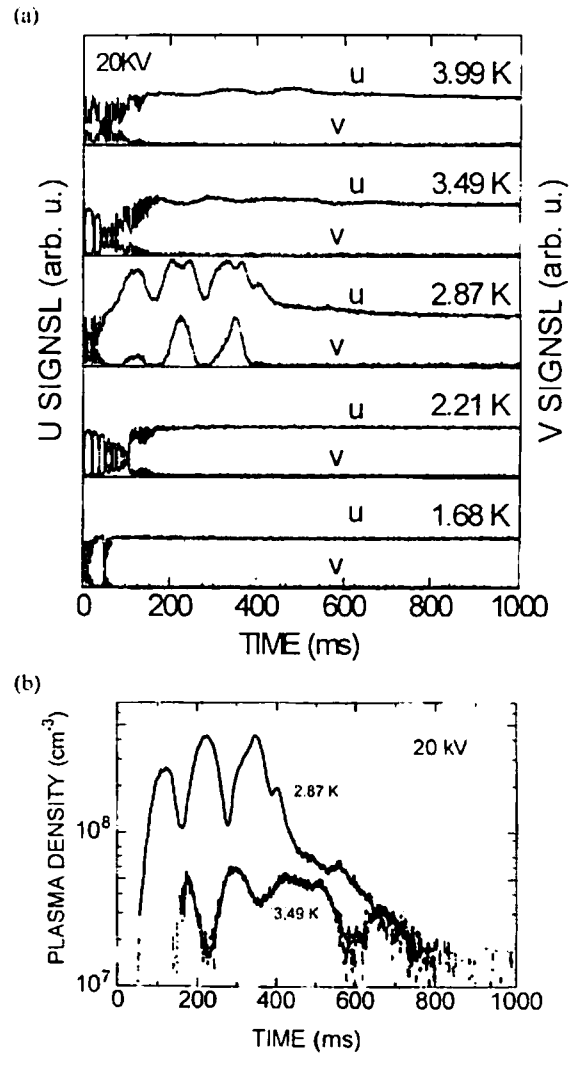

Fig. 4. Measured responses through the plasma cavity filled with liquid helium at saturated vapor pressure for various temperatures with applied voltage 20 kV. (a) Waveforms of signals u and v. (b) Calculated plasma density versus time for two temperatures 2.87 and 3.49 K.

T, agreeing with the previous work [10], and increases with gas pressure as expected for the ion–ion recombination coefficient given by Thomson's theory for tenuous gases [11].

2) Decaying Plasma in the Cavity Filled With Liquid Helium at T = 4.2–1.69 K: Next, the cavity is filled with LHe, and the signals u and v are measured. The experiments are carried out in LHe mostly at saturated vapor pressure under the condition that the gas volume above the free surface of LHe filling completely the cavity is isolated from the outer helium-gas-feeding tubing-connection by closing the valve. Since LHe in the cavity is in thermal equilibrium with the surrounding LHe in the dewar that is cooled down by evacuation, LHe in the cavity is maintained to have the saturated vapor pressure. The temperature of LHe in the cavity is measured precisely from the gas pressure above the free surface. Plasma density is calculated by (1) in which bare electrons are assumed to respond to the microwave fields. The signals u and v on the order of 200 ms after the pulsed discharge are observed with good reproducibility, while the plasma decays in much shorter period in the gas case in Figs. 2 and 3. The long time sustainment of the plasma may result from the slow diffusion of the localized plasma through LHe compared to the gas cases given in the previous sub-section. Fig. 4(a) shows the responses of the signals u and v through the plasma cavity for various temperatures with the applied discharge voltage of 20 kV. The plasma density is estimated to be on the order of 10^8 cm^{-3}, an approximate value in the late afterglow period of the pulsed discharge in LHe. Temporal evolutions of the plasma density calculated by (1) are shown in Fig. 4(b) for temperatures 2.87 and 3.49 K. The maximum density is attained at T = 2.87 K, while the plasma signals disappear below T = 2.3 K. The dependence of the u and v signals for various applied voltages in the case T = 2.87 K is shown in Fig. 5(a), and the corresponding plasma densities are shown in Fig. 5(b) for applied voltages 17, 19 and 20 kV. It is shown that the plasma density increases with the applied voltage. The range of observed plasma density is 10^7 – 10^9 cm^{-3} in the cavity, which is estimated with the assumption that the charged carriers responding to the microwave fields in the cavity are single electrons rather than ion clusters [6]–[8].

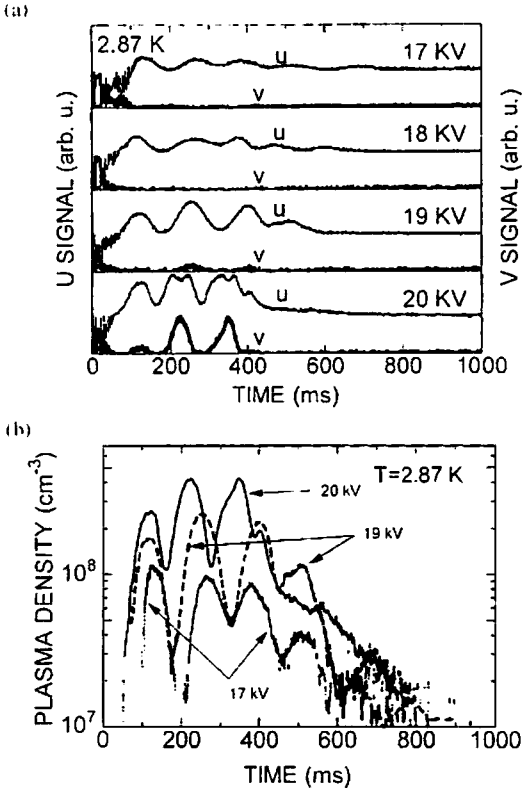

Fig. 5. Measured responses through the plasma cavity filled with liquid helium at saturated vapor pressure for various applied voltages. Liquid temperature is 2.87 K at saturated vapor pressure. (a) Waveforms of signals u and v. (b) Calculated plasma density versus time for three applied voltages 17, 19, and 20 kV.

IV. Analysis of Temporal Evolution of Localized Plasma in Liquid Helium

Simple three-dimensional analysis of localized decaying plasma in LHe is presented in this section. Recombination coefficients and mobility of ions in LHe available in the literature are reviewed and expected temporal evolution of the decaying plasma in LHe is analyzed numerically.

A. Properties of Charged Carriers in Liquid Helium

Properties of p- and n-ions in LHe have been studied by many researchers [12], revealing:) the p-ion in LHe to be a semi-macroscopic impurity object with radius of 0.6 nm and with effective mass 40 times that of a ^{4}He atom for the temperature range 1.2–4.2 K and 2) the n-ion in LHe to be a semi-macroscopic impurity object with radius 1–1.6 nm and with effective mass 240 times that of a ^{4}He atom [6]–[8], [13]. Ambient neutral ^{4}He atoms are attracted by a week dipole field of a core ^{4}He p-ion, forming a p-ion cluster or an ice-ball. On the other hand, a free electron in LHe is trapped inside a vacuum bubble which is explained by Pauli's exclusion principle. Because of the hydrodynamic nature, the electron in the bubble is called the n-ion. At 0.3 K and 24 atm, p- and n-ions can move without drag force when the velocities are below the Landau limit 46 m/s known to create a pair of rotons [14]. Large ion mobility was observed in a variety of experiments in LHe for higher temperatures and lower pressures with the ion velocity much smaller than the Landau velocity. So far, all of the experimental studies on ions in LHe have been restricted to direct current (dc) current densities much less than 10^{-6} A/cm^2 produced by a radio-isotope ion source [6]–[8], [15], [16] or dc field emission from a metal projection [14] immersed in LHe. The masses M_p and M_n of p- and n-ions are roughly $M_p = 40M(^4He) = 2.68 \times 10^{-25}$ kg and $M_n = 240M(^4He) = 1.61 \times 10^{-24}$ kg, respectively [6]–[8]. Since the mass of a p-ion is smaller than that of the n-ion, relatively mobile charged carriers that respond to the microwave field in our experiment may be mainly p-ions. In LHe, the responding p-ion has the mass M_p that is $M_p/M_e = 40 \times 4 \times 1837 = 2.9 \times 10^5$ times the mass M_e of a single electron. The range of observed plasma density may be 2.9×10^5 times larger than those in the plasma experiment in cryogenic helium gas shown in the previous subsection, because the observed plasma density n is proportional to mass M_p for a given plasma frequency.

The ion–ion recombination coefficient α in LHe was measured by Careri and Gaeta [15] for a temperature range 0.87–2.0 K at saturated vapor pressure, as shown by white squares in Fig. 6(a) where theoretical values are also shown. The measured α was found to agree with the conventional Langevin's theory shown by black circles for high pressure gases at 300 K, where the mean free paths of ions are much smaller than the average ion inter-particle distance. Thus, the recombination coefficient may be given by [9] $\alpha = e(\mu_p + \mu_n)/\varepsilon_0$, where μ_p and μ_n are the mobilities of the p- and the n-ions, and $\alpha(\mathrm{cm}^3/\mathrm{s}) = 1.81 \times 10^{-6}(\mu_p + \mu_n)$ with μ_p and μ_n in the unit of $\mathrm{cm}^2\mathrm{s}^{-1}\mathrm{V}^{-1}$. Using the data of the mobility by Schwarz, the black circles of α in Fig. 6(a) denoted by Langevin–Schwarz are obtained. White triangles in Fig. 6(a) are Harper's theory [17] of α in high pressure gases obtained in somewhat improved way rather than Langevin's theory and the results are around 1/4 times smaller than those of Langevin–Schwarz. The white triangles are denoted as Harper–Schwarz, since the data by Schwarz were again used. The values of α measured by Careri and Gaeta [15] are located just between two curves of Langevin–Schwarz and Harper–Schwarz. The mobility of p-ions in LHe is determined by the interactions of charged carriers with rotons, phonons and ^{3}He impurities that are the targets of scattering for the collisions [18]. These exitons play the role of neutral atoms to provide the mobility of ions in conventional gases. For T above 0.6 K, the dominant exitons in LHe are rotons, and Langevin's recombination coefficient is given by

$$\alpha(\mathrm{cm}^3/\mathrm{s}) = 1.4 \times 10^{-9} \exp(8.7/T) \qquad (3)$$

that is denoted as "theory of roton" by a broken line in Fig. 6(a). The measured recombination coefficient by Careri and Gaeta [15] agrees well with the broken line of roton for $T < 2.0$ K. We extend the recombination coefficient α given by (3) to the temperature range $T = 0.5$–2.17 K, although no experimental data measurements were available in the full range. The white circles at the left top corner of Fig. 6(a) are ion–ion recombination coefficients α given by Thomson's theory [11] for low gas pressure less than 1 atm such that mean free paths of ions are much larger than the average ion inter-particle distance. The ion–ion recombination coefficient is $\alpha \approx 10^{-2}$ cm^3/s around temperature $T = 0.5$ K as shown in Fig. 6(a).

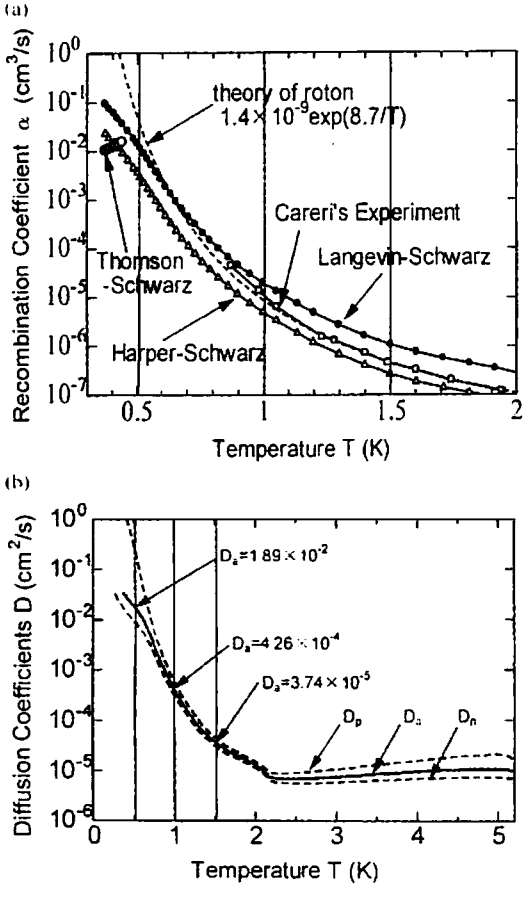

Fig. 6. Recombination and diffusion coefficients of ions in liquid helium calculated from known data in the literature. (a) Recombination coefficients versus temperature measured by Careri and Gaeta [15]. Other curves are theoretical values using the data of mobility of positive and negative ions measured by Schwarz [16]. (b) Free and ambipolar diffusion coefficients versus temperature calculated from the data of mobility measured by Schwarz [16].

Schwarz measured zero-field mobility of tenuous p- and n-ions in LHe at saturated vapor pressure [16]. The mobility of the p-ion at $T = 0.37$ K increases as much as 10^6 times the lowest values at 4.2 K, while the mobility of the n-ion at $T = 0.37$ K increases as much as 3×10^4 times the lowest values at 4.2 K. The ambipolar diffusion coefficient D_a of ions in LHe may be evaluated by $D_{p,n} = (kT/e)\mu_{p,n}$ or $D_{p,n}(\mathrm{cm}^2/\mathrm{s}) = 8.63 \times 10^{-5} T(K)\mu_{p,n}(\mathrm{cm}^2/\mathrm{Vs})$. Here, we assume $T_p = T_n = T$. The free diffusion coefficients $D_{p,n}$ as a function of temperature are shown by broken lines in Fig. 6(b). The ambipolar diffusion coefficient D_a may be given by [9]

$$D_a(\mathrm{cm}^2/\mathrm{s}) = \frac{\mu_n D_p + \mu_p D_n}{\mu_n + \mu_p} = 1.73 \times 10^{-4} T(K)\mu_a(\mathrm{cm}^2/\mathrm{Vs}) \quad (4)$$

where $1/\mu_a = 1/\mu_n + 1/\mu_p$ as given by Blanc's Law. The ambipolar diffusion coefficient D_a is shown by a solid curve in Fig. 6(b). It is evident that $D_n < D_a < D_p$, although these three diffusion coefficients are on the same order of magnitude for $T > 1.0$ K. As shown in Figs. 6(a) and 6(b), both D_a and α increase many orders of magnitude with the decrease in T from 2 to 0.5 K because of the nature of superfluidity.

B. Evolution of Localized Plasma in Liquid Helium

The localized plasma produced by a pulsed discharge in LHe is characterized by the high initial density and the temperature on the order of 10^{18} cm^{-3} and 3×10^4 K, respectively, surrounded by a gas layer [2], [5]. When the pulsed discharge is over, the plasma vanishes quickly, and some ions are implanted into LHe before they recombine [5]. Ions with temperature higher than the temperature of LHe will diffuse quickly and may distribute through LHe in the cavity.

Decay in density $n(r, t)$ of the localized plasma produced in LHe may be caused by recombination and diffusion losses as expressed by

$$\frac{\partial n}{\partial t} = -\alpha n^2 + D_a \frac{1}{r^2}\frac{\partial}{\partial r}\left(r^2 \frac{\partial n}{\partial r}\right) \quad (5)$$

where α and D_a are the recombination coefficient and the ambipolar diffusion coefficient, respectively. The differential equation (5) is solved numerically assuming the initial density distribution observed earlier in Fig. 3(a) in [5], namely, the distribution with the half half-width of 0.3 mm. First, we choose the coefficients α and D_a from Fig. 6 and set $\alpha = 1.2 \times 10^{-7}$ cm^3/s and $D_a = 1.0 \times 10^{-5}$ cm^2/s in a normal fluid case ($T_p = T_n = T = 1.2$ K), while $\alpha = 1.0 \times 10^{-5}$ cm^3/s, $D_a = 1.26 \times 10^{-4}$ cm^2/s in a superfluid case ($T_p = T_n = T = 1.0$ K). The results for both cases are shown in Fig. 7(a) and (b), respectively. As shown in Fig. 7(a), the effect of ambipolar diffusion becomes dominant for the density less than 10^{9} cm^{-3} at the time 100 s in the normal fluid, and 1~10 s in the superfluid case in Fig. 7(b). In our experiment, as shown in Figs. 4(b) and 5(b), however, the plasma density decays in less than 1 s. Such a disagreement between observed and expected decay times may be attributed to a difference in the diffusion coefficients between the experiment in Figs. 4(b) and 5(b), and the calculation in Fig. 7.

Next, we choose values of the diffusion coefficients from the following expression as

$$D_a = \frac{\frac{1}{2}\left(\frac{L}{2}\right)^2}{3T_d} \quad (6)$$

where $L = 5.6$ cm is the length of the cylindrical plasma container and $T_d = 0.2$ s is the delay time after the pulsed discharge. The decay time T_d in (6) is the time of signal arrival at the location of the antenna at $r = L/2$ from a point source of plasma at $r = 0$. The diffusion coefficient $D_a = 6.5$ cm^2/s obtained from (6) is found to agree with the observation in the decaying plasma in cryogenic gas shown in Fig. 8(a) of [4]. Fig. 8(a) in this paper shows the temporal evolution of the plasma density versus the radial distance r assuming $D_a = 6.5$ cm^2/s and $\alpha = 1.0 \times 10^{-7}$ cm^3/s. We note that plasma expands much faster than the expected results shown in Figs. 7(a) and (b). To see the effect of the diffusion coefficients on the plasma density at the antenna, we plot the plasma density at the antenna location $r = L/2 = 2.8$ cm, as a function of time by the solution of (5) with $\alpha = 0$

$$n = \frac{C}{(4\pi D_a t)^{\frac{3}{2}}} \exp\left(-\frac{r^2}{4D_a t}\right) \quad (7)$$

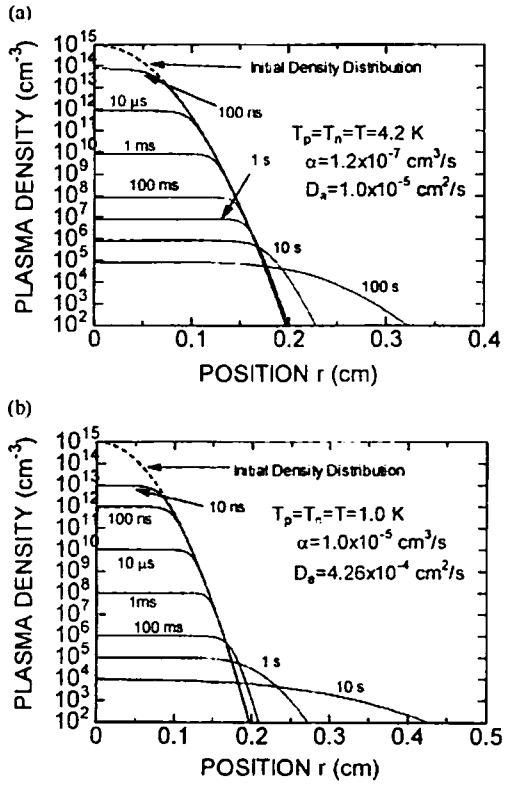

Fig. 7. Temporal evolution of localized cryogenic plasma in liquid helium with a diffusion coefficient calculated by (5). Here, an initial density profile measured by Kojima *et al.* [5] and recombination and diffusion coefficients shown, respectively, in Fig. 6(a) and (b) have been used. (a) Liquid helium at constant temperature $T = T_p = T_n = 4.2$ K (normal fluid) with saturated vapor pressure. (b) Liquid helium at constant temperature $T = T_p = T_n = 1.0$ K (superfluid) with saturated vapor pressure. Here T, T_p, and T_n are the temperature of liquid helium, p-ions, and n-ions, respectively.

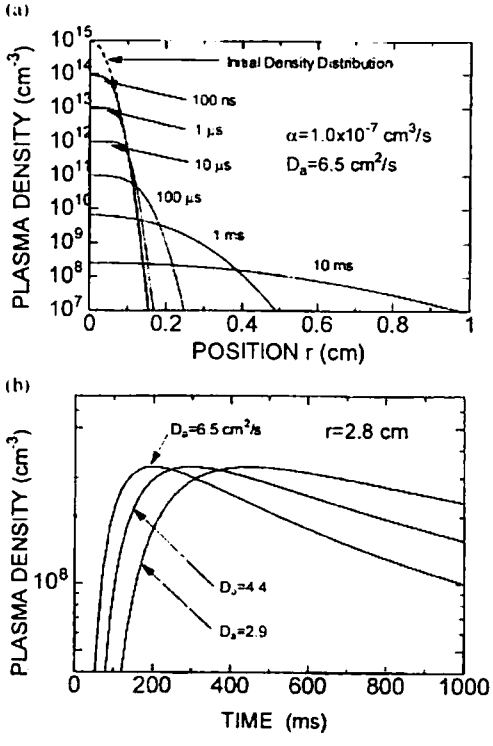

Fig. 8. Numerical solutions for the evolution of a localized plasma in liquid helium with assumed diffusion coefficients to fit the observed results in Figs. 4(b) and 5(b). (a) Temporal evolution of localized cryogenic plasma in liquid helium with initial density distribution measured by Kojima *et al.* [5]. Here, the recombination coefficient $\alpha = 1.0 \times 10^{-7}$ cm^3/s and ambiploar diffusion coefficient $D_a = 6.5$ cm^2/s are assumed. (b) Temporal evolution of plasma density, (7), at the position of the antennas $r = L/2 = 2.8$ cm from the point source of plasma discharge at $r = 0$ and $t = 0$. Recombination coefficient $\alpha = 0$ and ambiploar diffusion coefficients, $D_a = 6.5$, 4.4 and 2.9 cm^2/s are assumed. This figure is to be compared with those observed in Figs. 4(b) and 5(b).

where C is a constant. The origin $r = 0$ is taken at the electrode where the plasma is produced. Fig. 8(b) shows the plasma density as a function of time at the location $r = 2.8$ cm for $D_a = 2.9 \sim 6.5$ cm^2/s. The density becomes maximum at the time when $\partial n/\partial t = 0$ in (7) that results in (6), which corresponds to the delay time T_d. Fig. 8(b) would compare favorably with the experimental data, Fig. 4(b) and Fig. 5(b), in the time scale except the observed oscillatory nature with three or four peaks. The observed diffusion process takes place much faster than those expected from Fig. 7, where heavy p-ion mass was assumed. The temporal observation of the plasma density as shown in Figs. 4(b) and 5(b) might be understood by the loss process with the diffusion coefficient given by (6), rather than by (4). We might conclude that the ambipolar diffusion involves ions with mass of light single helium atom and bare electrons in LHe. The oscillatory nature of the plasma density observed in Fig. 4(b), as well as in Fig. 5(b) with a number of peaks remains to be solved.

V. Discussion and Conclusion

We have measured the density of the decaying plasma in LHe. The observed masses of charged carriers are estimated to be much smaller than those expected in [6]–[8]. We conclude that the recombination coefficient [15] and the mobility [16] measured previously at steady-state in drift tubes filled with LHe using dc ion source may not be applied to the transient state just after the pulsed discharge in the present experiment. Our microwave measurement is made using the principle of comparing the sensing frequency ω with plasma frequency $\omega_p = (ne^2/\varepsilon_0 m)^{1/2}$. For a given ω_p, the measured density n increases with mass m in (2). Assuming p-ions to be the responding charged carriers to the microwave field, the scales of density n in vertical axes in Figs. 4(b) and 5(b) would be 2.9×10^5 times larger than those shown in these figures. Although the exact masses of ions in LHe just after the high-voltage pulsed discharges have not been reported yet in any literature, it may be reasonable to estimate the density of charged carriers to be on the order of 10^8 cm^{-3} with the assumption of a single electron mass in the late afterglow period rather than 10^{13} cm^{-3} assuming heavy p-ions. The present experiment suggests that masses of charged carriers observed after the high-voltage pulsed discharge in LHe are much smaller than those of heavy ions in steady state measured in LHe [6]–[8]. It is conjectured that some finite time on the order of one second will need to form positive ion clusters or electron bubbles with full effective masses [6]–[8]. All the earlier experiments to measure the ion masses were made for charged carriers produced

by the steady-state ion sources. In other words, ions were created a long time before the measurements. Our measurement, however, is made just after the production of charged carriers in LHe. Our result does not exclude the possibility of the presence of heavy ions that could not be detected. The lower limit of temperature of LHe in our experiment is 1.69 K. Fig. 6(a) and (b) suggests that distinct features of cryogenic ions in LHe would appear around $T = 0.5$ K.

The present measurements of cryogenic afterglow plasma in LHe are carried out by a microwave cavity method. Additional measurements for localized low density plasma either by electrostatic probe or by wave propagation would be desirable to confirm the results in the present microwave measurements that lack spatial resolution. The Langmuir probe was used to determine the plasma characteristics in cryogenic afterglow plasma in LHe, giving a preliminary result of unexpected high temperature of charged carriers. Further efforts to improve accuracy of the measurements are under way.

In conclusion, charged carriers with masses smaller than the expected conventional values are observed in the transient plasma in LHe. Although the microwave cavity method may not detect the localized plasma precisely, our measurements to estimate the masses of ions in the cryogenic decaying plasma in LHe are reported for the first time in the literature. Study of cryogenic plasma in LHe including the time of formation of an ion cluster and an electron bubble with various effective masses is a new subject of research in plasma science. Distinct effects of superfluidity in cryogenic plasma in LHe near 0.5 K are to be clarified experimentally in the future. Theoretical and computational analyzes to elucidate the novel features of the cryogenic plasma in LHe should be promoted.

ACKNOWLEDGMENT

The authors would like to acknowledge Prof. A. W. DeSilva, University of Maryland, for reading the manuscript.

REFERENCES

[1] T. C. Killian, S. Kulin, S. D. Bergeson, L. A. Orozco, C. Orzel, and C. Rolston, "Creation of an ultracold neutral plasma," *Phys. Rev. Lett.*, vol. 83, no. 23, pp. 4776–4779, Dec. 1999.

[2] W. Qin, K. Minami, A. W. DeSilva, F. Tomimoto, and K. Sato, "Time-resolved spectroscopic measurements of plasmas after pulsed discharges in liquid helium," *Jpn. J. Appl. Phys.*, pt. 1, vol. 35, no. 8, pp. 4509–4515, 1996.

[3] ——, "Emission spectra from pulsed discharges in liquid helium," *Jpn. J. Appl. Phys.*, pt. 1, vol. 36, no. 7A, pp. 4474–4480, 1997.

[4] K. Minami, Y. Yamanishi, C. Kojima, M. Shindo, and O. Ishihara, "Very slowly decaying afterglow plasma in cryogenic helium gas," *IEEE Trans. Plasma Sci.*, vol. 31, no. 3, pp. 429–437, Jun. 2003.

[5] C. Kojima, K. Minami, W. Qin, and O. Ishihara, "Optical observation of localized plasma after pulsed discharges in liquid helium," *IEEE Trans. Plasma Sci.*, vol. 31, no. 6, pp. 1379–1383, Dec. 2003.

[6] A. J. Dahm and T. M. Sanders Jr., "Relaxation time, effective mass, and structure of ions in liquid helium," *Phys. Rev. Lett.*, vol. 17, no. 3, pp. 126–130, July 1966.

[7] J. Poitrenaud and F. I. B. Williams, "Precise measurement of effective mass of positive and negative charge carriers in liquid helium II," *Phys. Rev. Lett.*, vol. 29, no. 18, pp. 1230–1232, Oct. 1972.

[8] ——, "Erratum," *Phys. Rev. Lett.*, vol. 32, no. 21, p. 1213, May 1974.

[9] S. C. Brown, *Introduction to Electrical Discharges in Gases*. New York: Wiley, 1966, pp. 27–149.

[10] J. F. Delpech and J. C. Gauthier, "Electron-ion recombination in cryogenic helium plasmas," *Phys. Rev. A, Gen. Phys.*, vol. 6, no. 5, pp. 1932–1939, 1972.

[11] A. von Engel, *Ionized Gases*. Oxford, U.K.: Clarendon, 1955.

[12] P. V. E. McClintock, D. J. Meredith, and J. K. Wigmore, *Low-Temperature Physics: An Introduction for Scientists and Engineers*. London, U.K.: Blackie, 1992.

[13] P. E. Parks and R. J. Donnelly, "Radii of positive and negative ions in helium II," *Phys. Rev. Lett.*, vol. 16, no. 2, pp. 45–48, Jan. 1966.

[14] T. Ellis and P. V. E. McClintock, "The breakdown of superfluidity in liquid ^{4}He V. Measurement of the Landau critical velocity for roton creation," *Philos. Trans. R. Soc. London A, Math. Phys. Sci.*, vol. 315, pp. 259–300, 1985.

[15] G. Careri and F. Gaeta, "Ionic recombination in liquid helium," *Il Nuovo Cimento*, vol. 20, no. 1, pp. 152–160, 1961.

[16] K. W. Schwarz, "Charge-carrier mobilities in liquid helium at the vapor pressure," *Phys. Rev. A*, vol. 6, no. 2, pp. 837–844, Aug. 1972.

[17] W. R. Harper, "On the theory of the recombination of ions in gases at high pressures," *Proc. Camb. Phil. Soc.*, vol. 28, pp. 219–233, 1932.

[18] K. W. Schwarz and R. W. Stark, "Scattering of positive ions by elementary excitations in superfluid helium," *Phys. Rev. Lett.*, vol. 22, no. 24, pp. 1278–1280, 1969.

Kazuo Minami (M'98) was born in Japan, in 1938. He received the B.S. degree from Nagoya Institute of Technology, Nagoya, Japan, in 1962, the M.S. degree from Tokyo Institute of Technology, Tokyo, Japan, in 1964, and the Ph.D. degree from Nagoya University, in 1969, all in electrical engineering.

From 1986 to 2004, he was a Professor in the Department of Electrical and Electronic Engineering, Niigata University, Niigata, Japan. He is currently with Faculty of Engineering, Tokyo Denki University, Tokyo, Japan. His research interests include the generation of high-power microwave radiation and cryogenic plasmas in superfluid liquid helium.

Chikara Kojima was born in Japan, in 1978. He received the B.S. and M.S. degrees in electrical engineering from Niigata University, Niigata, Japan, in 2002 and 2004, respectively. He is currently toward the Ph.D. degree at Yokohama National University, Yokohama, Japan.

His research interests include cryogenic plasmas.

Takeo Ohira was born in Japan, in 1981. He received the B.S. degree in electrical engineering from Niigata University, Niigata, Japan, in 2004. He is currently working towards the M.S. degree at the Graduate School of Energy Science, Uji Campus, Kyoto University, Japan.

His research interests include cryogenic plasmas in liquid helium.

Osamu Ishihara (F'98) received the B.S. and M.S. degrees from Yokohama National University, Yokohama, Japan, in 1972 and 1974, respectively, and the Ph.D. degree in electrical engineering from the University of Tennessee, Knoxville, in 1977.

From 1977 to 1984, he was at the Plasma Physics Laboratory, University of Saskatchewan, Saskatoon, Canada. He was in the Faculty of Texas Tech University, Lubbock, from 1985 to 1999. He is currently Professor of Physics in the Faculty of Engineering at Yokohama National University, Yokohama, Japan. His research interests include plasma waves, instabilities, turbulence, complex plasmas, air plasmas, and ultracold plasmas.

Dr. Ishihara has been involved in organizing the IEEE International Conference on Plasma Science.

APPENDIX 2

Joint conference of 19th International Conference on Numerical Simulation of Plasmas (ICNSP) and 7th Asia Pacific Plasma Theory Conference (APPTC)

July 12-15, 2005

Nara-Ken New Public Hall, Nara, Japan

Book of Abstracts

Hosted by

National Institute for Fusion Science

Sponsored by

Japan Society for the Promotion of Science

Joint with

The US-Japan workshop on "New Development of Simulation Science"

And the Japan-Australia Plasma Theory and Computation Workshop

P1-65

Study of Decaying Plasma in Liquid Helium

Chikara Kojima, Osamu Ishihara and Kazuo Minami [1)]
Yokohama National University, Japan
1) Tokyo Denki University, Japan

1. Introduction

We produced cryogenic decaying plasma in liquid helium (LHe) as well as in cryogenic gas helium with temperature below 4.2 Kelvin by means of a pulsed discharge [1]. A plasma was produced in cryogenic helium gas in a TE_{011} mode S-band cavity with very long decay time on the order of 1 sec [1], while high-voltage pulsed discharge with needle electrodes in LHe produced the localized plasma with density more than 10^{18} cm^{-3} and electron and ion temperatures of a few eV [2]. Upon termination of the discharge, the plasma remained as long as on the order of 10 μsec in LHe. Some of ions and electrons remained longer in LHe before they recombine. Such a cryogenic plasma, or positive and negative ion mixture dissolved in LHe, is studied in detail.

2. Experiment

We apply the microwave cavity method to measure decaying plasma in LHe [3]. The schematic cross section of plasma cavity is shown in Figure 1. Plasma is produced in plasma cavity by means of a pulse discharge. Late afterglow plasma in an X-band cavity filled with LHe in the temperature range from 4.2 to 1.69 K is studied. Our microwave measurement is based on the principle of comparing the applied frequency ω with the cavity resonance frequency. The resonant frequency in the cavity will be shifted upward in the presence of plasma and the detected frequency shifting will determine the plasma density n through plasma frequency $\omega_p = (ne^2 / \varepsilon_0 m)^{1/2}$.

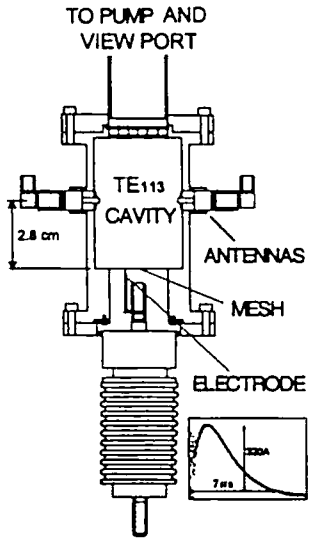

Figure 1. Cross section of plasma cavity

3. Results and Conclusion

A slow decaying plasma in LHe at a saturating vapor pressure with temperature above 2.3 K is detected as long as 200 ms after the discharge. Plasma density vs. time for two temperatures 2.87 and 3.49K is shown in Figure 2. The exact masses of ions in LHe just after the high-voltage pulsed discharges have not been reported yet in any literature. It is estimated that the reasonable density of charged carriers to be on the order of 10^8 cm^{-3} with the assumption of a single electron mass in the late afterglow period rather than 10^{13} cm^{-3} assuming a positive ion. The present experiment suggests that masses of charged carriers observed after the high-voltage pulsed

discharge in LHe are much smaller than those of ions in a steady state measured in LHe [4,5].

We conclude that masses of charged carriers measured previously at steady-state in drift tubes filled with LHe using DC ion source may not be applicable to the transient state just after the pulsed discharge in the present experiment. It is conjectured that some finite time on the order of one second will need to form positive ion clusters or electron bubbles with full effective masses [4,5]. We note that all the earlier experiments to measure the ion masses were made for charged carriers produced by the steady-state ion sources. Our measurement, however, is made just after the production of charged carriers in LHe. Our result does not exclude the possibility of the presence of heavy ions that could not be detected. Our estimated density based on the cavity method suggests an effective mass of ions much different from that expected by the conventional theory. A simple diffusion loss model for a temporal evolution of the localized plasma produced by the pulsed discharge in LHe reveals the presence of charged carriers with masses much lighter than those expected in LHe[3].

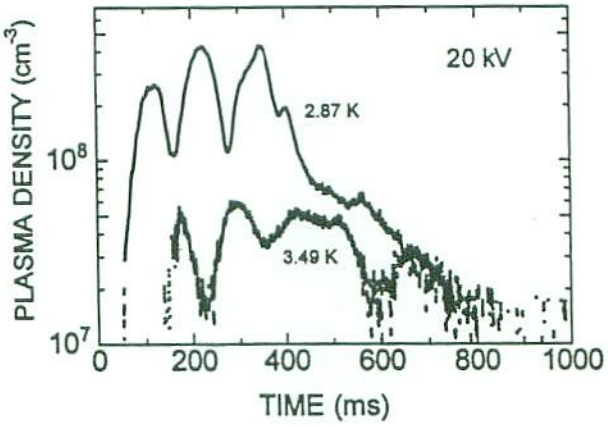

Figure 2. Plasma density vs. time for two temperatures 2.87 and 3.49 K

This work is supported in part by AOARD (Asian Office of Aerospace Research and Development), and by Grant-in-Aid for Scientific Research (c) (2) in Japan Society for Promotion of Science.

References

[1] K. Minami, Y. Yamanishi, C. Kojima, M. Shindo and O. Ishihara, "Very slowly decaying afterglow plasma in cryogenic helium gas," *IEEE Trans. Plasma Sci.*, vol. 31, no. 3, pp. 429-437, June 2003.

[2] C. Kojima, K. Minami, W. Qin and O Ishihara, "Optical observation of localized plasma after pulsed discharges in liquid helium," *IEEE Trans. on Plasma Sci.* vol. 31, no. 6, pp. 1379-1383, Dec. 2003.

[3] K. Minami C. Kojima, T.Ohira and O. Ishihara "Microwave measurement of Decaying Plasma in Liquid Helium," *IEEE Trans. Plasma Sci.*, Aug, 2005.

[4] J. Poitrenaud and F. I. B. Williams, "Precise measurement of effective mass of positive and negative charge carriers in liquid helium II," *Phys. Rev. Lett.*, vol. 29, no. 18, pp. 1230-1232, Oct. 1972.

[5] J. Poitrenaud and F. I. B. Williams, Erratum, *Phys. Rev. Lett.*, vol. 32, no. 21, pp. 1213, May 1974.

APPENDIX 3

Fall Meeting, Physical Society of Japan (2005.9.19-22, Kyoto)

(original in Japanese)

横国大．石原 修

日本物理学会 2005年秋季大会 プログラム

日本物理学会誌

BUTSURI

第60巻 8月増刊号（通巻653号）ISSN 0029-0181
昭和30年6月13日 第3種郵便物許可
平成17年8月5日発行 毎月5日発行
2005 VOL. 60
8月増刊号

大阪市立大学杉本キャンパス
（9月12日～9月15日）
リッツ・カールトン・ホテル
（9月18日～9月22日）
同志社大学京田辺キャンパス
（9月19日～9月22日）

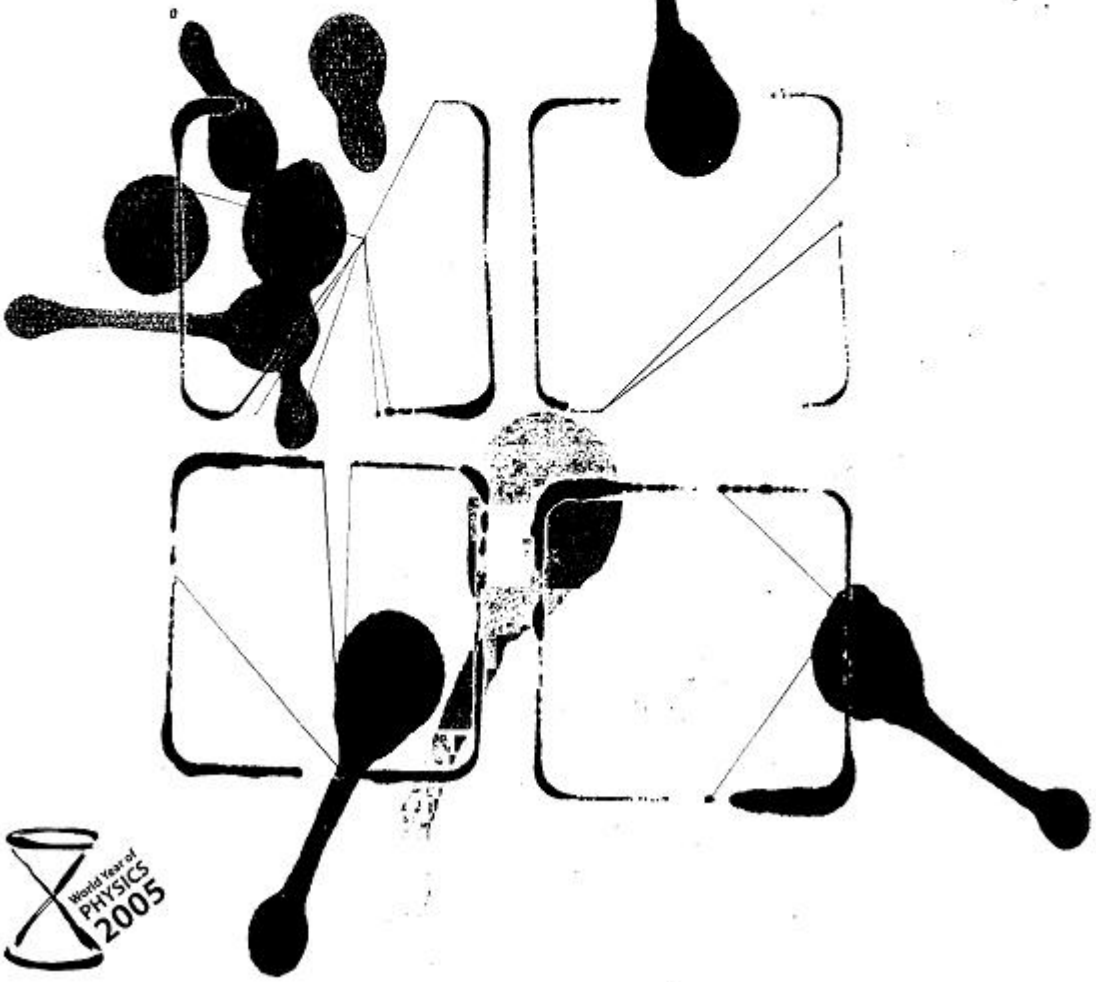

World Year of PHYSICS 2005

APPENDIX 1

21pWG-1

Observation of dust particles in a plasma under cryogenic environment

M. Shindo, C. Kojima, O. Ishihara
Yokohama National University

A complex plasma in a cryogenic environment is studied experimentally. A plasma is produced in a vapor of liquid helium by applying the low frequency AC voltage between plane electrodes. Fine acrylic particles are injected into a plasma. Fine particles are negatively charged because of the higher mobility of electrons than ions hitting on the surface of the particles. Electrons, ions and fine particles form a complex plasma where the overall charge neutrality is satisfied. The complex plasma is quite different from the ordinary plasma in a sense that the coupling constant of fine particles, defined by the ratio between the Coulomb interaction energy and the thermal energy of fine particles, is much larger than unity and fine particles are strongly coupled through the Coulomb interaction.

Figure 1 shows the experimental apparatus in which Liquid helium is in a double glass Dewar of 10 cm in diameter and 1m in length, and the liquid temperature is cooled down to 1K by evaporative cooling. The pressure at the upper part of the Dewar was about 300 Pa. The discharge electrodes of 5mm apart are placed about 20cm above the surface of liquid helium, while a mesh electrode and a plate electrode of 5 cm in diameter are placed below the discharge electrodes. The 10kHz AC voltage of 1kV was applied to the electrodes. The discharge electrodes are protected by a cylindrical insulator to suppress the rapid rise of the temperature of both Liquid helium and the vapor gas, while all the electrodes are in an acrylic tube of 5cm in diameter to confine the particles. The plasma diffuses toward the surface of Liquid helium through a 5mm hole in the lower electrode. Electron temperature decreases gradually toward the surface of Liquid helium. The acrylic particles of 5μm in diameter were dropped through the 5mm holes at the center of the upper electrode into the plasma. The He-Ne laser light irradiated though a 1cm-width slit on the silver plated glass Dewar confirmed the particles levitating 1cm above the plate electrode.

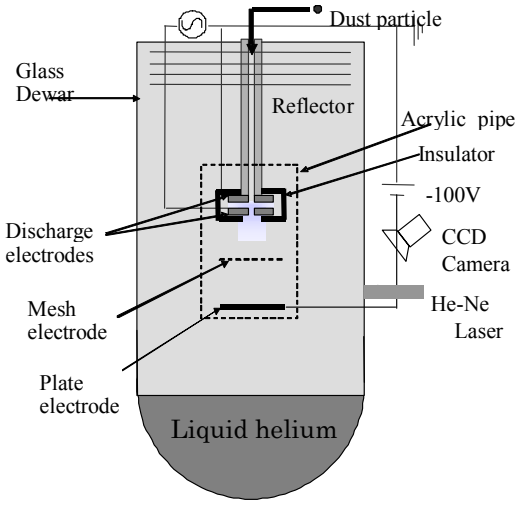

Fig.1 Schematic diagram of dust plasma apparatus in cryogenic condition.

This work is supported by Asian Office of Aerospace Research and Development.

22aWG-2

Plasma production in a cryogenic condition

C. Kojima, M. Kugue, T. Maezawa, M. Shindo and O. Ishihara
Yokohama National University

A steady production of a plasma in a cryogenic environment is studied experimentally. After a successful production of a plasma in a gas at the liquid helium temperature (below 4.2K) by a pulse discharge (20kV with a pulse width 7 μs)[1], our efforts are concentrated on producing a cold plasma for an extended period of time. Our attempt to produce a cryogenic plasma in a steady state is achieved by an electrical discharge (AC10kHz, ～1kV) in a vapor (300 Pa) above the liquid helium surface.

The electrical discharge in the vapor necessarily brings a heat in the environment resulting in the boiling of the liquid helium. To overcome the rise of the surrounding plasma temperature as well as the instability of the surface of the liquid helium, a special purpose discharge unit was developed as shown in Fig. 1 in which a region of plasma production is isolated from the surroundings by a small glass Dewar[2].

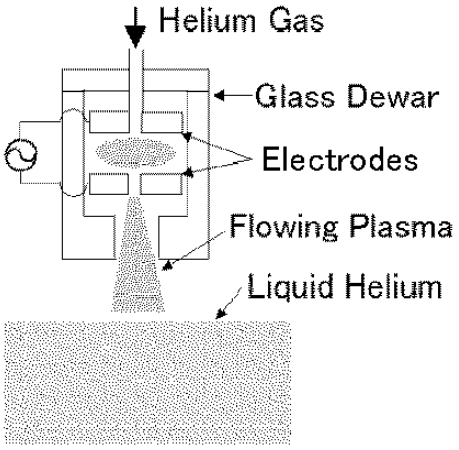

Fig.1 Schematic diagram of the discharge unit in the vapor of liquid helium.

Two identical plane discharge electrodes of 22 mm in diameter and 5mm in thickness have coaxial holes at the center through which the helium gas was fed from the upper hole. A plasma is produced by a discharge between the electrodes and the gas flow takes the plasma outside of the discharge region through the bottom hole.

The rise of the plasma temperature once outside of the glass Dewar is successfully suppressed and the plasma temperature decreases toward the surface of the liquid helium. The cold plasma in a steady state is thus produced.

This work is supported by Asian Office of Aerospace Research and Development.

[1] K. Minami, Y. Yamanishi, C. Kojima, M. Shindo and O. Ishihara, *IEEE Trans. Plasma Sci.*, vol. 31, no. 3, pp. 429-437, June 2003.
[2] H.Bauer, M.Beau, A.Bernhardt, B.Friedl, H.J.Reyher, *Phys. Lett. A*, vol.137, pp.217-224, 1989.

APPENDIX 4

Attractive force on like charges in a complex plasma

Osamu Ishihara[a)]
Faculty of Engineering, Yokohama National University, 240-8501 Yokohama, Japan

Noriyoshi Sato
Emeritus, Graduate School of Engineering, Tohoku University, Sendai 980-8579, Japan

(Received 11 May 2005; accepted 2 June 2005; published online 7 July 2005)

Electrostatic attractive force between dust particles in a complex plasma with ion flow is studied. It is shown that there is an attractive force between a pair of dust particles along the ion flow as well as perpendicular to the ion flow. The attractive force perpendicular to the flow results from a release of thermodynamic free energy in charged fine particles, while an attractive force associated with the wake potential acts on a pair of dust particles aligned with the ion flow. Recent experimental observation of the sharp boundary of a void in a complex plasma is interpreted as a result of the attractive force. © *2005 American Institute of Physics*. [DOI: 10.1063/1.1978467]

A void structure, characterized by a dust-free ordered state with a sharp boundary in a dusty plasma, was observed in experiments in microgravity conditions[1] as well as in ground-based laboratory plasmas.[2] A theory was presented to explain the void formation based on the balance of the electrostatic force and the ion drag force acted on a dust particle.[3] Since accumulated observations of the void in a complex plasma challenged the theory, alternative theories including thermophoretic force,[2,4] phenomenological theory,[5] and nonlinear theory[6,7] have been presented. Meanwhile, the ion drag force reevaluated recently by taking the screened Coulomb potential into account is revealed to be much stronger than that estimated earlier.[8] Most recent experimental observation confirmed the role of the ion drag force for the formation of the void.[9] Voids have been observed not only in a complex plasma, but also in colloidal suspensions where an attractive pair interaction was considered.[10,11] Like-charge attraction is a recent subject in a plasma as well as in a colloid.[12,13] In this Letter, we consider a complex plasma, where macroparticles are embedded in a fully ionized plasma and the system is thermodynamically closed, and we show that a like-charge attraction could align dust particles along the equipotential line on a void boundary perpendicular to the ion flow in the complex plasma, while the ion flow will produce the wake potential behind dust particles along the direction of the flow.

We consider a complex plasma in which N dust particles are embedded in a fully ionized collisionless plasma. We neglect the gravitational effect, as is the case in microgravity experiments. The radius of a spherical dust particle, a, is assumed to be much smaller than the Debye shielding length λ_D. The charge density of the complex plasma is given by

$$\rho(\mathbf{x}) = Z_d e \sum_{j=1}^{N} \delta(\mathbf{x}-\mathbf{x}_j) + e n_i(\mathbf{x}) - e n_e(\mathbf{x}), \tag{1}$$

where $Z_d e$ is the charge of a dust particle located at $\mathbf{x}=\mathbf{x}_j$, $n_i(\mathbf{x})$ is ion density, and $n_e(\mathbf{x})$ is electron density. A charge neutrality condition is given by

$$\overline{n_e} - \overline{n_i} = N Z_d / V, \tag{2}$$

where V is the volume occupied by a complex plasma, $\overline{n_i} = \int d^3x n_i(\mathbf{x})/V$ and $\overline{n_e} = \int d^3x n_e(\mathbf{x})/V$. The electrostatic potential produced by N dust particles at a position $\mathbf{x}$ at time t is given by

$$\phi(\mathbf{x},t) = \sum_{\mathbf{k}} e^{i\mathbf{k}\cdot\mathbf{x}} \int_{\mathrm{Br}} \frac{d\omega}{2\pi} e^{-i\omega t} \phi(\mathbf{k},\omega), \tag{3}$$

where Br indicates the Bromwich integration path and

$$\phi(\mathbf{k},\omega) = \frac{i4\pi Z_d e}{V k^2 \omega \varepsilon(\mathbf{k},\omega)} \sum_{j=1}^{N} e^{-i\mathbf{k}\cdot\mathbf{x}_j}, \quad \mathrm{Im}\ \omega > 0. \tag{4}$$

The plasma in consideration is assumed to be characterized by a dielectric constant

$$\varepsilon(\mathbf{k},\omega) = 1 + \frac{k_{De}^2}{k^2} - \frac{\omega_{pi}^2}{(\omega - \mathbf{k}\cdot\mathbf{v}_f)^2}, \tag{5}$$

where $\mathbf{v}_f$ is the velocity of the flowing ions, $k_{De}^2 = 4\pi \overline{n}_e e^2/\kappa T_e$, $\omega_{pi}^2 = 4\pi \overline{n}_i e^2/m_i$ with the electron temperature T_e, the ion mass m_i, and the Boltzmann constant κ. The dielectric constant (5) characterizes the plasma where the ion flow is dominant and the collisions are negligible. We note that the collective modes expressed by Eq. (5) damp for the wave numbers $k > k_{De}$. The poles of Eq. (3) with $\phi(\mathbf{k},\omega)$ by Eq. (4) are located at $\omega=0$ and $\omega=\omega(\mathbf{k})$, where $\varepsilon[\mathbf{k},\omega(\mathbf{k})] = 0$ and $\omega(\mathbf{k}) = \mathbf{k}\cdot\mathbf{v}_f \pm \omega_{\mathbf{k}}$. Here we introduced $\omega_{\mathbf{k}} = \omega_{pi} k/\sqrt{k^2+k_{De}^2}$. We obtain the electrostatic potential as

$$\phi(\mathbf{x}) = \phi_0(\mathbf{x}) + \phi_1(\mathbf{x}) + \phi_w(\mathbf{x}), \tag{6}$$

where[14]

[a)]Electronic mail: oishihar@ynu.ac.jp

$$\phi_0(\mathbf{x}) = \frac{4\pi Z_d e}{V}\sum_{j=1}^{N}\sum_{\mathbf{k}}\frac{e^{i\mathbf{k}\cdot(\mathbf{x}-\mathbf{x}_j)}}{k^2+k_{De}^2},$$

$$\phi_w(\mathbf{x}) = \frac{4\pi Z_d e}{V}\sum_{j=1}^{N}\sum_{\mathbf{k}}\frac{e^{i\mathbf{k}\cdot(\mathbf{x}-\mathbf{x}_j)}}{k^2+k_{De}^2}\frac{\omega_{\mathbf{k}}^2}{(\mathbf{k}\cdot\mathbf{v}_f)^2-\omega_{\mathbf{k}}^2}, \tag{7}$$

and $\phi_1(\mathbf{x})$ is the potential contribution from the pole $\omega=\omega(\mathbf{k})$ which characterizes the strong interaction of a dust particle with the collective plasma mode. The potential $\phi_w(\mathbf{x})$ is known to be responsible for producing an oscillating wake potential behind each dust particle along the ion flow.[14–18] For a single dust particle ($N=1$), the contributions from the potential $\phi_0(\mathbf{x})$ and $\phi_1(\mathbf{x})$ were shown to be canceled by the part of the potential $\phi_w(\mathbf{x})$ resulting in the wake potential existing only behind the isolated dust particle in the supersonic ion flow.[14] The wake potential is the source of the attractive force between dust particles along the ion flow. Because of such an attractive force, dust particles align themselves along the direction of the ion flow. We now show that for a multiparticle system ($N\geqslant 2$), the potential $\phi_0(\mathbf{x})$ is responsible to produce an attractive force between dust particles perpendicular to the ion flow.

The electrostatic energy in the presence of a supersonic ion flow is given by

$$E = \int\frac{|\nabla\phi(\mathbf{x})|^2}{8\pi}d^3x \approx \frac{2\pi Z_d^2 e^2}{V}\sum_{i,j}\sum_{\mathbf{k}}\frac{k^2}{(k^2+k_{De}^2)^2}e^{-i\mathbf{k}\cdot(\mathbf{x}_i-\mathbf{x}_j)}. \tag{8}$$

The energy depends explicitly on Z_d and the coupling parameter $\eta(\equiv e^2)$, and implicitly on $\bar{n}_e$ and $\bar{n}_i$ through Z_d and k_{De}. We note that the electrostatic energy is induced by a pair displacement $\mathbf{x}_i-\mathbf{x}_j$, a novel feature of a multiparticle system. Such a displacement necessarily introduces the volume change in the system through the relationship $G=F+PV$, where G is the Gibbs free energy and F is the Helmholtz free energy. The thermodynamic excess energy (Gibbs energy) thus may be evaluated as

$$G = \sum_{s=e,i}\left(\bar{n}_s\frac{\partial}{\partial\bar{n}_s}+\bar{n}_s\frac{\partial Z_d}{\partial\bar{n}_s}\frac{\partial}{\partial Z_d}\right)\int_0^{\eta}\frac{E(\eta')}{\eta'}d\eta' = \frac{2\pi Z_d^2 e^2}{V}\sum_{i,j}\sum_{\mathbf{k}}\left[\frac{1}{k^2+k_{De}^2}+\frac{k^2}{(k^2+k_{De}^2)^2}\right]e^{-i\mathbf{k}\cdot(\mathbf{x}_i-\mathbf{x}_j)}. \tag{9}$$

Here we use $\bar{n}_e\partial(k^2+k_{De}^2)^{-1}/\partial\bar{n}_e=-k_{De}^2(k^2+k_{De}^2)^{-2}$ and $\bar{n}_e\partial Z_d/\partial\bar{n}_e+\bar{n}_i\partial Z_d/\partial\bar{n}_i=Z_d$. The $\mathbf{k}$ summation may be evaluated through the integration

$$\sum_{\mathbf{k}}\xrightarrow[V\to\infty]{}\frac{V}{(2\pi)^3}\int_0^{\infty}k^2dk\int_0^{\pi}\sin\theta\,d\theta\int_0^{2\pi}d\varphi,$$

where $\mathbf{k}$ is chosen to be along the z axis, θ and φ are polar angles of $\mathbf{x}_i-\mathbf{x}_j$ with respect to the z axis. The excess energy becomes

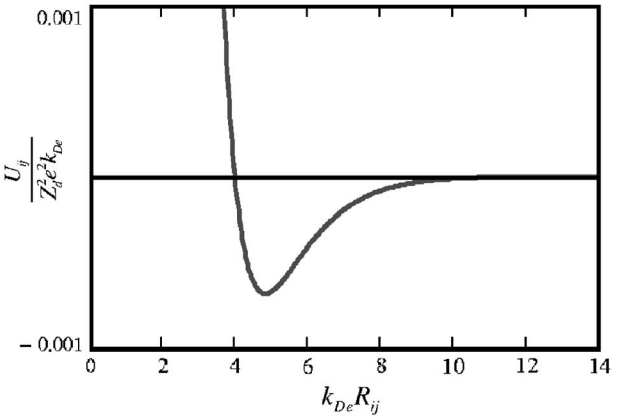

FIG. 1. Normalized potential as a function of the normalized interparticle distance.

$$G=\sum_{i,j}U_{ij},\quad U_{ij}=\frac{2Z_d^2e^2}{R_{ij}}\left(1-\frac{1}{4}k_{De}R_{ij}\right)e^{-k_{De}R_{ij}}, \tag{10}$$

where $R_{ij}=|\mathbf{x}_i-\mathbf{x}_j|$ is the interparticle distance, and the force acting on a dust pair is given by

$$F_{ij}=-\frac{\partial U_{ij}}{\partial R_{ij}}=\frac{2Z_d^2e^2}{R_{ij}^2}\left(1+k_{De}R_{ij}-\frac{1}{4}k_{De}^2R_{ij}^2\right)e^{-k_{De}R_{ij}}. \tag{11}$$

Figure 1 shows the normalized potential as a function of the normalized interparticle distance. The potential becomes minimum at $R_{ij}=4.83k_{De}^{-1}\equiv R_0$.

In a complex plasma experiment with parallel electrode plates, a potential has its maximum at the center of the plasma between electrodes. The equipotential lines close themselves making circles or deformed ellipsoidal lines in the cross section.[19] Thus the electric field $\mathbf{E}$ is directing outward from the center driving the electrons inward, while producing the flux of ions outward. Negatively charged dust particles are pushed inward to the center by the electric force, $\mathbf{F}_E=Z_de\mathbf{E}$, while the ion drag force, $\mathbf{F}_{\text{ion}}=m_i\int\mathbf{v}[\sigma_c(v)+\sigma_s(v)]vf_i(\mathbf{v})d^3v$, pushes dust particles from the center toward the outer region.[9] Here $f_i(\mathbf{v})$ is the ion distribution function, and the collection and the scattering cross sections are given by $\sigma_c(v)=\pi a^2(1+2b_0/a)$, $\sigma_s=4\pi b_0^2\ln[(b_0+\lambda_D)/(b_0+a)]$, respectively, where $b_0=Z_de^2/m_iv^2$.[20] Due to the balance of the two forces, dust particles characterized by the charge Z_de find their positions on an equipotential line. Some deviation of positions may be expected by the presence of other forces like neutral drag force, gravitational force, and Coulomb force.[21] Each dust particle on the equipotential line will be accompanied by aligned dust particles along the ion flow due to the wake potential, resulting in the void structure in the central part of the plasma. Dust particles of equal charges are positioned on the same equipotential line perpendicular to the direction of the ion flow and are subject to the force given by Eq. (11). Figure 2 describes the contour plot of the potential around a dust particle superimposed on the wake potential along the ion flow with Mach number $M=2$. The solid-black three circles are dust particles on an equipotential line, while the white circular band around a dust particle in the middle

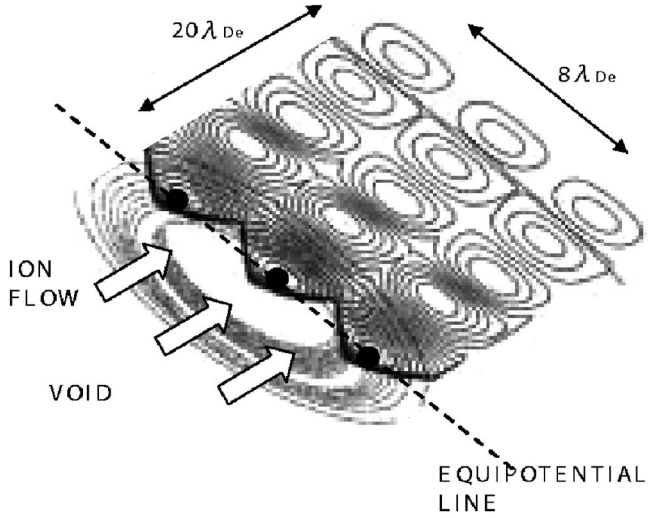

FIG. 2. Contour plot of the potential around dust particles in the ion flow. Three dust particles are shown by solid black circles. Wake potentials are shown in the direction of the ion flow behind the particles and the equipotential lines due to the particle in the middle are also shown. The two neighboring particles are located on the potential dips created by the middle particle.

shows the presence of a potential minimum with a radius R_0. The neighboring two dust particles on an equipotential line are settled at the minimum potential created by the dust particle in the center with the interparticle distance of R_0. The interparticle distance perpendicular to the flow is independent of the Mach number, while the supersonic ion flow produces the pattern of wake potential. With a smaller Mach number, the distance between potential minimums along the flow behind a dust particle becomes smaller.[14] It is straightforward to calculate the interparticle distance by including the finite radius a of a dust particle in a dust density as $Z_d e \Sigma \delta(|\mathbf{x}-\mathbf{x}_i|-a)/4\pi a^2$. The interparticle distance is then given by $R_{ij}=(1+a\coth k_{De}a)(1+\sqrt{1+2/(1+k_{De}a\coth k_{De}a)})$, as was first discussed in the context of colloids.[22]

In conclusion, the electrostatic attractive force between like charges in a complex plasma, where charged macroparticles are embedded in a fully ionized plasma, is shown to be responsible for the sharp boundary formation associated with a void which is prompted by the ion drag force. The attractive force may be interpreted as a release of thermodynamic free energy among charged fine particles in the presence of ion flow, while the attractive force associated with the wake potential may be interpreted as a result of phonon exchange in the presence of ion flow in a complex plasma.[16] The measurement of interparticle distances may be used to estimate plasma parameters. The interparticle distance perpendicular to the boundary will provide the ion flow velocity, while the interparticle distance along the boundary will provide the Debye screening length. Although the exact plasma parameters at the boundary of the void may be difficult to measure, some typical interparticle distance of small grains with radius on the order of a few micrometers has been reported to be on the order of 0.1 mm in the range of a few ion Debye lengths and less than an electron Debye length in microgravity conditions with $n_e \approx n_i \sim 10^9$ cm^{-3}, $T_e \approx 3$ eV, and $T_i \approx 0.03$ eV.[23] It should be noted that the proposed void structure is operative in a complex plasma which is thermodynamically closed. In our analysis we have neglected, as is shown by the dielectric constant (5), the effect of ion-neutral collisions and thermal spread in ion velocities which are commonly present in laboratory experiments. Since a weakly ionized plasma with neutrals and finite ion temperature is characterized by an open dissipative system in dust plasma experiments, some deviation on the interparticle distance for attractive force to occur may be expected.

This research was supported by Japan Society for the Promotion of Science Grant-in-Aid for Scientific Research (B) under Grant No. (2) 1 6 3 4 0 1 7 9.

[1] G. E. Morfill, H. M. Thomas, U. Konopka, H. Rothermel, M. Zuzic, A. Ivlev, and J. Goree, Phys. Rev. Lett. **83**, 1598 (1999); A. P. Nefedov, G. E. Morfill, V. E. Fortov, H. M. Thomas, H. Rothermel, T. Hagl, A. V. Ivlev, M. Zuzic, B. A. Klumov, A. M. Lipaev, V. I. Molotkov, O. F. Petrov, Y. P. Gidzenko, S. K. Krikalev, W. Shepherd, A. I. Ivanov, M. Roth, H. Binnenbruck, J. A. Goree, and Y. P. Semenov, New J. Phys. **5**, 33.1 (2003); Y. Hayashi, Jpn. J. Appl. Phys., Part 1 **44**, 1436 (2005).
[2] G. Praburam and J. Goree, Phys. Plasmas **3**, 1212 (1996); D. Samsonov and J. Goree, Phys. Rev. E **59**, 1047 (1999); H. Rothermel, T. Hagl, G. E. Morfill, M. H. Thoma, and H. M. Thomas, Phys. Rev. Lett. **89**, 175001 (2002).
[3] R. P. Dahiya, G. V. Paeva, W. W. Stoffels, E. Stoffels, G. M. W. Kroesen, K. Avinash, and A. Bhattacharjee, Phys. Rev. Lett. **89**, 125001 (2002).
[4] J. Goree, G. E. Morfill, V. N. Tsytovich, and S. V. Vladimirov, Phys. Rev. E **59**, 7055 (1999).
[5] K. Avinash, Phys. Plasmas **8**, 2601 (2001).
[6] K. Avinash, A. Bhattacharjee, and S. Hu, Phys. Rev. Lett. **90**, 075001 (2003).
[7] D. Jovanovic and P. K. Shukla, Phys. Lett. A **308**, 369 (2003).
[8] S. A. Khrapak, A. V. Ivlev, G. E. Morfill, and S. K. Zhdanov, Phys. Rev. Lett. **90**, 225002 (2003).
[9] M. Kretschmer, S. A. Khrapak, S. K. Zhdanov, H. M. Thomas, G. E. Morfill, V. E. Fortov, A. M. Lipaev, V. I. Molotkov, A. Ivanov, and M. V. Turin, Phys. Rev. E **71**, 056401 (2005).
[10] D. G. Grier and J. C. Crocker, Phys. Rev. E **61**, 980 (2000).
[11] N. Ise, Proc. Jpn. Acad., Ser. B: Phys. Biol. Sci. **78**, 129 (2002).
[12] V. N. Tsytovich, Comments Plasma Phys. Controlled Fusion **15**, 349 (1994); V. N. Tsytovich and G. E. Morfill, Plasma Phys. Rep. **28**, 171 (2002).
[13] T. M. Squires and M. P. Brenner, Phys. Rev. Lett. **85**, 4976 (2000).
[14] O. Ishihara and S. V. Vladimirov, Phys. Plasmas **4**, 69 (1997).
[15] M. Nambu, S. V. Vladimirov, and P. K. Shukla, Phys. Lett. A **203**, 40 (1995); S. V. Vladimirov and O. Ishihara, Phys. Plasmas **3**, 444 (1996).
[16] O. Ishihara and S. V. Vladimirov, Phys. Rev. E **57**, 3392 (1998).
[17] D. Winske, W. Daughton, D. S. Lemons, and M. S. Murillo, Phys. Plasmas **7**, 2320 (2000); M. Lampe, G. Joyce, G. Ganguli, and V. Gavrishchaka, *ibid.* **7**, 3851 (2000).
[18] K. Takahashi, T. Oishi, K. Shimonai, Y. Hayashi, and S. Nishino, Phys. Rev. E **58**, 7805 (1998).
[19] M. R. Akdim and W. J. Goedheer, Phys. Rev. E **65**, 015401(R) (2001).
[20] S. A. Khrapak, A. V. Ivlev, G. E. Morfill, and H. M. Thomas, Phys. Rev. E **66**, 046414 (2002).
[21] O. Ishihara, Phys. Plasmas **5**, 357 (1998).
[22] I. Sogami and N. Ise, J. Chem. Phys. **81**, 6320 (1984).
[23] G. E. Morfill, M. Rubin-Zuzic, H. Rothermel, A. V. Ivlev, B. A. Klumov, H. M. Thomas, U. Konopka, and V. Steinberg, Phys. Rev. Lett. **92**, 175004 (2004); V. V. Yaroshenko, B. M. Annaratone, S. A. Khrapak, H. M. Thomas, G. E. Morfill, V. E. Fortov, A. M. Lipaev, V. I. Molotkov, O. F. Petrov, A. I. Ivanov, and M. V. Turin, Phys. Rev. E **69**, 066401 (2004).